Leaf accumulation of atmospheric dust : biomagnetic, morphological and elemental evaluation using SEM, ED-XRF and HR-ICP-MS

Reference:
Castanheiro Ana, Hofman Jelle, Nuyts Gert, Joosen Steven, Spassov Simo, Blust Ronny, Lenaerts Silvia, De Wael Karolien, Samson Roeland.- Leaf accumulation of atmospheric dust : biomagnetic, morphological and elemental evaluation using SEM, ED-XRF and HR-ICP-MS
Atmospheric environment : an international journal - ISSN 1352-2310 - 221(2020), 117082
Full text (Publisher's DOI): https://doi.org/10.1016/J.ATMOSENV.2019.117082
To cite this reference: https://hdl.handle.net/10067/1654580151162165141

Leaf accumulation of atmospheric dust: biomagnetic, morphological and elemental evaluation using SEM, ED-XRF and HR-ICP-MS

Ana Castanheiro [a, 1, *], Jelle Hofman [a, b, 1], Gert Nuyts [c], Steven Joosen [d], Simo Spassov [e], Ronny Blust [d], Silvia Lenaerts [f], Karolien de Wael [c], Roeland Samson [a]

[a] Laboratory of Environmental and Urban Ecology, Department of Bioscience Engineering, University of Antwerp, Belgium

[b] Solutions4IoT Lab, Imec, High Tech Campus 31, 5656 AE Eindhoven, The Netherlands (present address)

[c] AXES Research Group, Department of Chemistry, University of Antwerp, Belgium

[d] Systemic Physiological and Ecotoxicological Research (SPHERE), Department of Biology, University of Antwerp, Belgium

[e] Laboratory for Environmental Magnetism, Geophysical Centre of the Royal Meteorological Institute, Dourbes, Belgium

[f] Sustainable Energy, Air and Water Technology Purification (DuEL), Department of Bioscience Engineering, University of Antwerp, Belgium

* Corresponding author: University of Antwerp, Groenenborgerlaan 171, V5.16, 2020, Antwerp, Belgium. Phone number: (+32) 032653569. E-mail address: Ana.Castanheiro@uantwerpen.be (A. Castanheiro)

[1] Equal contribution.

Abstract

Atmospheric dust deposition on plants enables the collection of site-specific particulate matter (PM). Knowing the morphology and composition of PM aids in disclosing their emitting sources as well as the associated human health risk. Therefore, this study aimed for a leaf-level holistic analysis of dust accumulation on plant leaves. Plant species (ivy and strawberry) with distinct leaf macro- and micro-morphology were exposed during three months at a moderate road traffic site in Antwerp, Belgium. Leaves collected every three weeks were analyzed for their magnetic signature, morphology and elemental content, by a combination of techniques (biomagnetic analyses, ED-XRF, HR-ICP-MS, SEM). Dust accumulation on the leaves was observed both visually (SEM) and magnetically, while the metal enrichment was limited (only evident for Cr) and more variable over time. Temporal dynamics during the second half of the exposure period, due to precipitation events and reduction of atmospheric pollution input, were evidenced in our results (elements/magnetically/SEM). Ivy accumulated more dust than strawberry leaves and seemed less susceptible to wash-off, even though strawberry leaves contain trichomes and a rugged micromorphology, leaf traits considered to be important for capturing PM. The magnetic enrichment (in small-grained, SD/PSD magnetite particles), on the other hand, was not species-specific, indicating a common contributing source. Variations in pollution contributions, meteorological phenomena, leaf traits, particle deposition (and encapsulation) *versus* micronutrients depletion, are discussed in light of the conducted monitoring campaign. Although not completely elucidative, the complex, multifactorial process of leaf dust accumulation can better be understood through a combination of techniques.

Keywords

Atmospheric dust deposition • PM leaf accumulation • Biomonitoring • Environmental magnetism • ED-XRF • HR-ICP-MS

1. Introduction

Air pollution monitoring using accumulation surfaces of green elements (*e.g.* leaves) is recurrently used as a rapid, yet reliable approach to explore habitat quality in cities and to identify contamination hot spots, mostly in terms of particulate matter (PM) pollution (*e.g.* Castanheiro et al., 2016; Dzierżanowski et al., 2011; Kardel et al., 2011; Mo et al., 2015; Popek et al., 2013; Sawidis et al., 2011; Tomašević et al., 2005; Wang et al., 2013). The micro-morphological attributes of plant leaves, with sticky epicuticular waxes, irregular structure and topography, also often containing trichomes, promote the deposition and accumulation of atmospheric particulates on their surface (Beckett et al., 2000; Grote et al., 2016; Liu et al., 2012a; Weerakkody et al., 2018) by gravitational sedimentation, impaction, interception and diffusion (Litschke and Kuttler, 2008). Besides trapping PM (mitigation action) or impacting local pollutant's dispersal and dilution (aerodynamic action), urban greening allows for a close study of PM chemical and physical characteristics under the influence of *e.g.* spatial/temporal variations and local/regional emissions (monitoring action) (*e.g.* Baldacchini et al., 2017).

Despite legislative and regulatory efforts to reduce PM levels such as for instance the inclusion of PM guidelines in the Gothenburg Protocol (UNECE, 2012), atmospheric PM remains a serious issue in developed and developing countries alike. Since 2000, anthropogenic emissions of fine particulate matter (≤ 2.5µm; $PM_{2.5}$) have decreased by 28% in Europe. However, in 2013-2015 ca. 82% of the urban population was still exposed to concentrations above the World Health Organization (WHO) $PM_{2.5}$ guideline (10 µg m^{-3} annual mean); for coarse PM (≤ 10 µm; PM_{10}), more than half of the population faced concentrations exceeding the WHO limit (20 µg m^{-3} annual mean) (EEA, 2017a, 2017b). These scenarios are even more worrying in emerging countries, where fast growing populations and industrialization are inevitably less sustainable; globally 9 out of 10 people breath air exceeding the WHO's air quality guidelines (WHO, 2018). Both short- and long-term exposure to atmospheric PM have been associated with *e.g.* cardiovascular and respiratory diseases and lung cancer mortality (Dockery and Pope, 1994; Pope et al., 2002). Oxidative stress and inflammation are the main mechanistic precursors of PM-induced health effects (Breysse et al., 2013; Moretti et al., 2019; Schwarze et al., 2006). In addition to total PM mass or concentration values, the particle size and composition are key factors as they differently affect human health and can reveal contributing emission sources. Particle number, size distribution (Vu et al., 2015), traffic- or combustion-related PM (Künzli et al., 2000; Laden et al., 2000), associated metals, organic compounds or biological species (Harrison and Yin, 2000; Schwarze et al., 2006) are among the components of interest.

A range of analytical methods is nowadays available for characterizing *e.g.* filter-collected PM, such as energy dispersive X-ray fluorescence (ED-XRF) and high-resolution inductively coupled plasma mass spectrometry (HR-ICP-MS). These two methods differ in terms of sample preparation and detection limits (Galvão et al., 2018, and references therein). ED-XRF allows for a non-destructive, cost-effective and straightforward determination of chemical elements on leaf specimens. This is even possible in relatively small concentrations since the main vegetal constituents (C, N, H, O) are considered transparent to X-rays (Marguí et al., 2009). On the other hand, inductively coupled plasma mass spectrometry (ICP-MS) requires samples in a liquid state to be pumped into a sample introduction system, after which they are subjected to a series of physico-chemical transformations before reaching the plasma state at high temperatures (Houk et al., 1980; Przybysz et al., 2014; Thomas, 2004). Such complex and onerous analytical routine results in the destruction or alteration of the samples, despite offering a higher detection capability compared to ED-XRF. The coupled use of ED-XRF and HR-ICP-MS for multi-element analysis has been reported before for aerosol samples collected on *e.g.* Teflon and quartz fiber filters (Okuda et al., 2013; Yatkin et al., 2011). Yet, to our knowledge, this is the first study where both techniques are applied on leaves to evaluate the accumulated dust composition. Such evaluation can be supplemented by magnetic analysis, which has proven to be a reliable and efficient tool to capture pollution gradients and sources (Baldacchini et al., 2017; Castanheiro et al., 2016; Hofman et al., 2017; Maher et al., 2008; Matzka and Maher, 1999).

Atmospheric dust deposition on leaves is mainly influenced by plant species (evergreen or deciduous, wax composition), specific leaf structure (leaf size, shape, roughness, trichomes), meteorological conditions (air humidity, rainfall, wind speed) and source-specific particle features (*e.g.* particle size distribution) (Chen et al., 2017; Dzierżanowski et al., 2011; Janhäll, 2015; Litschke and Kuttler, 2008; Mo et al., 2015). And so, leaf accumulation of dust also enables the collection of site-specific PM. Previous studies have investigated seasonal or temporal variation of PM leaf accumulation gravimetrically (*e.g.* Dzierżanowski et al., 2011; Przybysz et al., 2014; Sgrigna et al., 2015; Sæbø et al., 2012), magnetically (*e.g.* Lehndorff et al., 2006; Hofman et al., 2014a) and through microscopy (*e.g.* Wang et al., 2015). However, they mostly focused in comparing the end to the start of the growing season. In some cases, chemical-based techniques were also applied but to a rather small selection of samples (*e.g.* ICP-MS on three replicates per plants species, as in Przybysz et al., 2014) or on homogenized leaf material (*e.g.* ICP-MS or ED-XRF on leaf pulverized powders, as in De Nicola et al. (2008) and Kardel et al. (2018)). In the present study, we aimed for a leaf-level comprehensive analysis of atmospheric dust accumulation over time. Leaves from two plant species (ivy (*Hedera sp.*) and strawberry (*Fragaria sp.*)) with distinct leaf macro- and micro-morphology, exposed to similar conditions, were investigated throughout a period of three months. The magnetic signature, morphology and elemental content of the leaf accumulated dust was investigated by the combination of biomagnetic analysis, ED-XRF, ICP-MS and scanning electron microscopy (SEM). The study objectives were: a) to investigate the temporal leaf accumulation and composition of atmospheric dust throughout a period of three months, b) to relate the observed accumulation to different leaf characteristics or traits, and c) to evaluate how the various analytical techniques perform on delivering insight into the process of leaf dust accumulation.

2. Materials and methods

2.1 Leaf collection and sample preparation

Three ivy (*Hedera sp.*) and three strawberry (*Fragaria sp.*) plants were obtained from a nursery on May 12, 2017 (Garden Center Claes, Edegem, Belgium). After collection of blank (non-exposed) leaves (0w), the six plants were planted together in all-purpose potting soil, inside a robust plastic box (polypropylene; 43 x 36 x 26 cm, length x width x height). The box was perforated at the bottom to allow for water drainage and subsequently placed next to an air quality monitoring station (42R817) of the Flemish Environment Agency (VMM). This monitoring station (Groenenborgerlaan; 42R817; 51˚10'38.17" N, 4˚25'4.64" E), at ca. 100 m distance from the Campus Groenenborger of the University of Antwerp, Belgium, is located in a residential area with moderate car traffic, with the nearest traffic road at 10 m from the test plants. The land use class of the monitoring station is defined as sub-urban, with car traffic being the main locally contributing pollution source. Air quality and meteorological data can be found in SI.1 and Figure S.1. Since the biomonitoring campaign was carried out in summer period, plants were watered once a week to prevent soil drought stress. The watering was done avoiding any physical contact with the leaves.

Leaf collection was conducted every three weeks during a period of three months; consecutively on June 2 (3w), June 23 (6w), July 14 (9w) and August 4 (12w), 2017. Leaves were sampled at ca. 35-60 cm height from the ground, at a distance of at least 10-15 cm, from the soil in the box, in order to avoid direct soil contamination and to standardize any potential influence from resuspension of the potted soil or of the soil at the test site. Twelve leaves of each species (*i.e.* four leaves per plant) were collected per sampling point and subsequently divided in two groups: leaves 1-6 were punched with a metallic puncher (48 mm in diameter) to obtain suitable, homogenous leaf sizes for elemental analysis by ED-XRF and HR-ICP-MS; leaves 7-12 were used for biomagnetic and SEM analyses. Leaves 7 and 12 were cut in half and punched (10 mm in diameter) twice to collect adaxial and abaxial leaf samples for SEM. While leaves 1-6 had a constant surface area of ca. 18.1 cm^2 after being punched, the leaf surface area of leaves 7-12 was determined using a leaf area meter LI-3100C (Licor Biosciences, USA). Prior to the analyses, leaf samples 1-6 were kept in the fridge (4˚C), while leaves 7-12 were dried at 35°C for at least three days in a drying cabinet (Memmert, Germany).

2.2 Leaf surface elemental composition: ED-XRF and HR-ICP-MS

Leaf samples 1-6 were analyzed for their elemental composition via ED-XRF and HR-ICP-MS. First, leaf samples were analyzed by ED-XRF for the elements range Na – Bi, on both their adaxial and abaxial surface sides. For both plant species (ivy and strawberry), element concentrations of non-exposed, blank leaves (0w) were subtracted from the concentrations of the exposed leaves. Whenever elements were highly abundant and variable (with high relative standard deviation) in the blank leaves, high quantification limits were observed and it was not possible to accurately determine their concentrations. Concentrations found for elements Mg, Al, Mn and Zn were below the detection or quantification limits (additional information about the detection limits in SI.2). Samples were measured using a PANalytical Epsilon5 (UK) which has a 600 W Gd anode tube and is equipped with several secondary targets. The following parameters were used for the analyses of (i) Mg-Sn: tube voltage of 25 kV, current of 24 mA, live time of 500 s and a Ti secondary target; (ii) Ti-Ba: 75 kV, 8 mA, 1000 s and Ge secondary target; and (iii) Se-Bi: 100 kV, 6 mA, 1000 s and Mo secondary target, in the samples. The same parameters were used for the analyses of the blank leaves, but with three times the live time. Spectra were fitted using bAxil (BrightSpec, Belgium), after which net peak intensities were obtained and compared to all blank measurements. Quantification was performed by using sensitivity coefficients which were determined by measuring thin reference films and using a thin-film approximation allowing the concentrations (ng cm^{-2}) to be determined. This approximation is only fully correct for exogenous elements deposited on the leaf surface, whereas for all other elements the information depth needs to be considered. As an indication, we have calculated theoretical information depths using leaf composition from literature (*e.g.* Hobbie et al., 2006) and an average leaf density of 0.25 g cm^{-3} (Poorter et al., 2009). The calculated information depths were 60-850 µm (Na-Sc); 0.6-1 mm (Ru-Sn); 2-8 mm (Ti-Ga), 2-5 mm (Sb-Er); 1-4 cm (Ge-Nb) and 7-18 mm (Tm-Bi). Although these are estimates, it is clear that for elements with Z > 21 (Sc), the full leaf thickness (or a substantial part of it) is analyzed. In such cases, variations on thickness and bulk composition of leaves will have an influence on the X-ray response; thus, only if exogenous elements are detected, the ED-XRF quantification can be correctly performed. Secondly, leaf samples were individually transferred to acid washed 50 mL glass bottles with 15 mL of ultrapure water (0.055 µS cm^{-1}; Milli-Q, Merck, USA), which were then placed on an orbital shaker (GFL 3015, Germany) for 10 minutes at 180 rpm. The selected shaking time was previously tested on collected leaves of both plant species (ivy and strawberry). The conductivity of the water solutions achieved a plateau after 3 minutes of shaking, suggesting the stagnation of ions leached from the leaves, and therefore, of dust removal. The resulting washing solutions were collected and acidified with concentrated HNO_3 (Trace Metal Grade, Fisher Scientific, USA) for HR-ICP-MS analysis. The concentrations of elements Na, Mg, Al, Si, K, Ca, Ti, V, Cr, Mn, Fe, Co, Ni, Cu, Zn, As, Rb, Sr, Mo, Rh, Pd, Ag, Cd, Sb, Tl, Pb and U were determined. From those elements, concentrations of Rh, Pd, Tl and U were all below the method quantification limit ($1x10^{-3}$ µg L^{-1}, equivalent to ca. $6x10^{-5}$ µg L^{-1} cm^{-2}). The elements determined by the two techniques, namely, Si, K, Ca, Ti, Cr, Fe, Cu, Rb, Sr, Pb, were defined as ‘common elements’.

2.3 Leaf magnetic analyses

After drying, leaf samples 7-12 were stored at room temperature awaiting magnetic analysis. On the day of analysis, the leaf dry mass (mg) was measured using a S-234 analytical balance (Denver Instrument, USA; 0.1 mg precision), after which the samples were individually wrapped in cling film and packed in 6.7 cm^3 sample containers. Leaf samples were then analyzed for their low-field magnetic susceptibility and their anhysteretic and isothermal remanent magnetization (ARM and IRM, respectively). The magnetic susceptibility k, which illustrates how easily the sample material can get magnetized (Thompson and Oldfield, 1986), was measured using a Bartington MS2B system (Bartington Instruments, UK). ARM and IRM were measured using an Agico JR-6 magnetometer (Agico Ltd., Czech Republic). The ARM is the remanent magnetization acquired by superposing a small steady direct current (DC) magnetic field with an alternating current (AC) (Evans and Heller, 2003). While the AC field amplitude establishes which particles are involved in the magnetization process depending on their coercivity, the DC field (also named bias field) intensity controls the degree to which those particles are magnetized. Different AC/DC combinations (80mT/80µT, 100mT/40µT, 100mT/100µT, 200mT/100µT and 200mT/500µT) were performed for ARM acquisition using a LDA5/PAM1 system (Agico Ltd., Czech Republic). Highest ARM values were reached at 200mT/500µT ($ARM_{200/500}$). So, this field combination was used in further magnetic ratios, as well for calculating ARM susceptibility (χ_{ARM}), *i.e.* the ARM normalized for the DC bias field. IRM is acquired by imposing strong DC magnetic fields; when the applied field leads the sample to saturation, this is called saturation IRM, *i.e.* SIRM. The application of consecutively increasing DC fields until reaching saturation and subsequent demagnetization through the use of reverse fields can be used to characterize the type and grain size of magnetic particles present (Evans and Heller, 2003). In our study, IRM acquisition curves were obtained from consecutive field applications with intensities 1T, -1T, 10mT, 20mT, 40mT, 50mT, 60mT, 70mT, 80mT, 90mT, 100mT, 120mT, 150mT, 200mT, 250mT, 300mT, 500mT and 1T, using a Molspin pulse magnetizer (Molspin Ltd., UK). In order to gain insight on the magnetic grain size and the contribution of low/high coercivity magnetic minerals, additional magnetic indicators were produced from the magnetic properties measured, namely S-ratio ($SIRM/IRM_{-300}$), HIRM ($0.5(SIRM+IRM_{-300})$) and ARM/SIRM. More information on environmental magnetic analysis for monitoring atmospheric pollution can be found in the review of Hofman et al. (2017).

Magnetic intensities (ARM, IRM), expressed in mA m^{-1}, were corrected for the sample container volume (6.7 cm^3) and normalized for leaf surface area (in cm^2), yielding values expressed in A. The mass-specific magnetic susceptibility (χ_{mass}) was obtained by dividing the magnetic susceptibility (k, dimensionless) by the leaf dry mass and correcting it for the sample container volume, being expressed in m^3 kg^{-1}. The contribution of empty sample containers with cling foil (sample blank) was assessed for all measurements and subtracted from the magnetic signal of the corresponding leaf samples.

2.4 Leaf morphology and visualization: SEM

Each leaf sample punch (of 10 mm in diameter) was fixed on an aluminum pin stub, using conductive double-sided tape, and left to dry at room temperature for at least three days. Leaf punches were subsequently vacuum coated with carbon (ca. 20 nm thick layer; Leica EM ACE600, Germany) and analyzed with a field emission gun – environmental scanning electron microscope (FEG-ESEM) equipped with an energy dispersive X-Ray (EDX) detector (FEI Quanta 250, USA; at AXES and EMAT research groups, University of Antwerp), using an accelerating voltage of 20 kV, a take-off angle of 30°, a working distance of 10 mm, a sample chamber pressure of 10^{-4} Pa and a 3.6 spot size. All samples (adaxial and abaxial from leaves 7 and 12 after collection at 0w, 3w, 6w, 9w and 12w) were explored for their leaf micro-characteristics and leaf-surface deposited particles, for which illustrative secondary electron (SE) images were taken from two opposite locations (*e.g.* left and right) in the sample at magnifications 200x, 500x and 2500x.

2.5 Data analysis

Differences in leaf surface area and dry mass between ivy and strawberry plants were tested by using a one-way analysis of variance (ANOVA). Visual (histogram and qq plots) and statistical (Shapiro-Wilk normality test) methods were used to assess normality of the magnetic and elemental concentrations per monitored plant species (ivy and strawberry leaves). Results were transformed logarithmically to comply with normality assumptions, however, this did not ensure that the concentrations of all elements followed a normal distribution, due to inter-leaf variability even within the same plant and same exposure conditions. Measured elemental concentrations and magnetic parameters were tested against exposure time by using linear regression fit, while differences between the two plant species were investigated using ANOVA or non-parametric testing (Mann-Whitney or Kruskal Wallis tests) whenever variables were not normally distributed even after transformation. Where applicable, Spearman Rank correlation tests were applied to evaluate associations between different variables. Principal component analysis (PCA) was performed to explore the contribution of different elements in the accumulated leaf dust. Data was processed using Microsoft Excel 2016 and statistical analyses were conducted in JMP Pro 14 (SAS Institute Inc., 2018).

3. Results and Discussion

3.1 Leaf macro- and micro-morphology

Both (log-transformed) leaf dry mass and surface area showed to be significantly different ($p < 0.001$) between the two studied plant species. Ivy leaves were on average broader and heavier (35.2 ± 7.2 cm^2, 356.3 ± 93.7 mg; n = 30) than strawberry leaves (22.2 ± 5.4 cm^2, 135.3 ± 39.5 mg; n = 30) (Table S.1). These leaves, collected every three weeks during a period of three months (Figure 1), showed an increase in their dry mass with exposure time for ivy ($p = 0.005$, $R^2 = 0.25$, n = 30), while changes in the leaf surface area over time were only significant for strawberry ($p = 0.037$, $R^2 = 0.15$, n = 30). In terms of epicuticular wax structure, ivy leaves are characterized as platelets while strawberry leaves present wax platelets on the adaxial surface and very dense wax rodlets on the abaxial side (Barthlott et al., 1998; Kim et al., 2009). The micromorphology of strawberry leaves appeared more rugged than for ivy leaves, where an undulated topography is present (Figures S.2, S.3). A similar micromorphology and wax structure is observed on both leaf surfaces of ivy, with a high stomatal density on the abaxial side and absence of stomata on the adaxial side. For strawberry, a comparable micromorphology but distinct wax structures are found between both leaf sides, with long trichomes and stomata present on the abaxial side only.

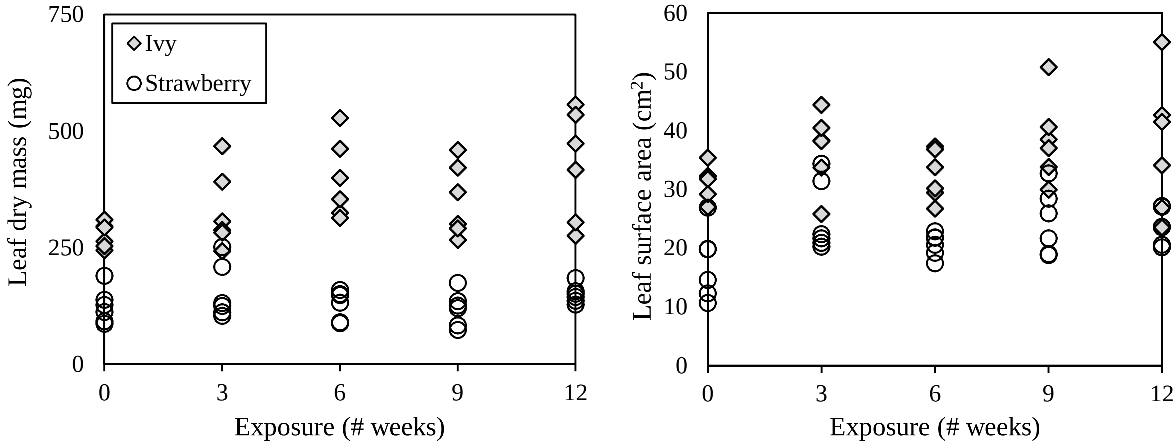

Figure 1 – Evolution of leaf dry mass (left) and surface area (right) of ivy and strawberry leaves collected throughout the exposure period (in weeks).

3.2 Leaf surface elemental composition

Predominant elements determined by ED-XRF included Si, Cl, Fe and Pb on both ivy and strawberry leaves (Tables S.2, S.4). Concentration ranges for Si (a major crustal component) and Pb (traffic-related) were very comparable between ivy and strawberry leaves, with slightly higher concentrations for ivy. Fe (crustal and traffic-related) was found in more than five times higher concentrations on ivy leaves than on strawberry. On the other hand, strawberry leaves showed to be almost nine times more effective in retaining Cl (a sea salt tracer) in comparison with ivy. Elements Ti, Cr, Cu, Br, Rb and Sr were also frequently measured on ivy leaves, but rarely on strawberry leaves (Table S.4). While Ti, Rb and Sr are associated with crustal resuspension, metals Cr and Cu can be derived from exhaust and non-exhaust road traffic (Amato et al., 2011, 2013; Vercauteren et al., 2011). Emissions of Br have been associated with marine contribution while anthropogenic sources include vehicle emissions, pesticides and chemical manufacturing (Lammel et al., 2002). Element concentrations determined by ED-XRF ranged from 6 $ng.cm^{-2}$ (*e.g.* Cr, Br) to more than 25,000 $ng.cm^{-2}$ (Cl, K, Ca) (Table S.2). It was found that Fe and Si ($p < 0.022$) accumulated more on ivy than on strawberry leaves, while the opposite was true for elements Sr and Cl ($p < 0.006$). The concentrations throughout the entire exposure period only increased significantly for Cl and Sr on ivy leaves ($p = 0.008$, $R^2 = 0.19$, $n = 15$; $p = 0.039$, $R^2 = 0.43$, $n = 23$). Such increases were observed for both leaf sides, although loosing significance for Sr when tested for each leaf side separately. The observed variability between leaves from the same species and exposure time was larger than expected (Table S.4), and concentrations were frequently below detection and/or quantification limits, from blank leaves to leaves exposed for three months. ED-XRF offers many advantages for multi-element, non-destructive analysis, which can be performed directly on the sample, at relatively low cost and with rapid output. Still, drawbacks are present caused by the heterogeneity of plant material due to chemical and physical matrix effects (Marguí et al., 2009). Particularly when samples do not meet the condition of thin-film, self-absorption effects arise that complicate the process of matrix calibration required for quantitative analysis (Bilo et al., 2017). Sample grinding or pelletization can be used to reduce such matrix effects (*e.g.* Marguí et al., 2005; Kardel et al., 2018), yet this was not possible in our study as the leaves analyzed via ED-XRF were subsequently used for ICP-MS determination.

An assessment was also made of the elements present on the non-exposed leaves, as this pre-exposure conditions can have an effect on the concentrations estimated for the exposed leaves. In general, the elements Al, P, S, Cl, K, Ca, Ti, Mn, Fe, Cu, Zn, Br, Rb and Sr, were present in all blank leaves (for both ivy and strawberry, both leaf surfaces) (Figure S.4), of which K, Ca, Mn and Fe were the most abundant elements. As mentioned (section 2.3), for elements with $Z < 22$ (*e.g.* Si, Cl) the information depth is less than the leaf thickness. Differences in the adaxial and abaxial analyses can, thus, be expected for those elements in case they are deposited heterogeneously on the leaf surfaces. For all other elements, in which the information depth is larger than the leaf thickness, both surfaces, and in fact the entire leaf depth, are analyzed by ED-XRF. Testing leaf surface side as a potential influencing factor for dust accumulation, revealed significantly higher accumulations of Cl for ivy ($p = 0.029$) and strawberry ($p = 0.015$), and Si for strawberry ($p = 0.002$), at the upper (adaxial) side compared to the lower (abaxial) leaf surface. The adaxial and abaxial concentrations as measured were compared against the overall leaf concentrations, *i.e.* obtained by averaging the adaxial and abaxial (element-specific) concentrations whenever both were available. This comparison revealed no differences regarding the analyzed ivy leaves, while for strawberry leaves, the averaged concentrations in Si differed from the abaxial values ($p = 0.047$).

The quantification on the exposed leaves of elements which were not detected on the blank leaves strongly suggests those elements to originate from the accumulation of atmospheric dust. This was the case for Ti, Cr and Pb. While the content in Ti and Cr in the blank leaves was unclear, Pb was absent on the blanks, but frequently detected on the exposed leaves (Table S.6). The Pb concentrations showed a similar temporal pattern for both leaf sides of each species, and also quite consistent for both ivy and strawberry. The highest yet more variable Pb concentrations were measured after six and twelve weeks of exposure (Figure S.5). The largest amount of rain (57 mm) was registered in the time interval between six and nine weeks of exposure, with 9w leaves being subject to double amounts of rain compared to the 6w leaves. The second largest precipitation period was between nine and twelve weeks (48 mm). While the precipitation between 9w and 12w was evenly distributed over the three weeks, for the period 6w – 9w a great peak of ca. 25 mm was registered only two days before the sampling of leaves 9w (Figure S.1). Most probably this rain event has removed some of the leaf accumulated dust by wash-off. Chen et al. (2017) observed that $PM_{2.5}$ removal from the leaf surface by wash-off was correlated with the amount of $PM_{2.5}$ accumulated on the leaf before a simulated rain event, and influenced by plant species and rainfall duration. During our exposure campaign, atmospheric PM_{10} and $PM_{2.5}$ concentrations were, as expected, negatively influenced by precipitation ($p = 0.0009$, Spearman's $\rho = -0.35$; $p = 0.039$, $\rho = -0.22$, respectively) due to atmospheric wash-out, and by wind speed ($p < 0.0001$, $\rho = -0.42$; $p = 0.0004$, $\rho = -0.37$). Higher wind speeds result in the dispersion and dilution of pollutants (Kgabi and Mokgwetsi, 2009) in both particulate and gaseous ($p < 0.0001$, $\rho = -0.55$ for NO_2) forms (Table S.7). PM concentrations were positively correlated with air temperature (PM_{10}, $p < 0.0001$, $\rho = 0.48$; $PM_{2.5}$, $p = 0.0003$, $\rho = 0.38$) while relative humidity (being inversely related to air temperature) showed to have a negative influence, mainly on the coarse fraction of PM (PM_{10}, $p = 0.0002$, $\rho = -0.39$; $PM_{2.5}$, $p = 0.36$). The latter confirms previous findings that moisture aids in the deposition of atmospheric particles by promoting their (condensational) growth in particle size (Jayamurugan et al., 2013; Litschke and Kuttler, 2008). The influence of air temperature, on the other hand, is rather complex since it greatly depends on the climate zone and diurnal/nocturnal variations, it has an inverse impact on relative humidity, and indirectly affects the emission of pollutants due to *e.g.* heating/cooling needs.

Leaf concentrations measured by ICP-MS are usually performed on pulverized or powdered samples (*e.g.* Alfani et al., 1996; De Nicola et al., 2013). However, this preparation procedure allows no distinction between the dust accumulated on the leaf surface (leaf-deposited particles) and the dust that becomes entrained on the leaves (leaf-encapsulated or in-wax particles). Nonetheless, leaf-encapsulated particles can amount to or even surpass the quantity of leaf-deposited particles, depending on plant species and particle size fraction (Dzierżanowski et al., 2011; Song et al., 2015). Moreover, such sample preparations are unable to exclude the intrinsic, natural leaf tissue elements. The element concentrations were, in our study, derived from the surface washing solution of collected leaves, with values ranging from 0.01 $ng.cm^{-2}$ (*e.g.* V, Co, Mo, Ag) up to more than 5,000 $ng.cm^{-2}$ (K, Ca) (Tables S.3, S.5). Most measured elements were detected on both ivy and strawberry leaves, but concentrations were always significantly higher for ivy than for strawberry leaves for Na, Ca, Fe, Cu, Cd ($p < 0.001$), Mg, Zn ($p = 0.001$), Mn ($p = 0.005$), Sb ($p = 0.006$) and Pb ($p = 0.042$). Plant leaves subject to traffic conditions compared to a traffic-poor background location are known to get enriched in trace metals such as Cr, Fe, Cu and Pb (De Nicola et al., 2008, 2013; Maher et al., 2008), although temporal dynamics of such leaf accumulation are less studied. Log-transformed concentrations showed to decrease or increase with exposure time depending on the elements and differently for ivy and strawberry plant leaves. For ivy (n = 25), decreasing concentrations in Al ($R^2 = 0.17$), Ti ($R^2 = 0.31$), Zn ($R^2 = 0.31$), Rb ($R^2 = 0.19$, n = 24), Sr ($R^2 = 0.25$), Sb ($R^2 = 0.16$), and increasing concentrations in Mg ($R^2 = 0.35$), Cr ($R^2 = 0.35$), Mn ($R^2 = 0.37$), Co ($R^2 = 0.26$) were observed ($p < 0.05$). For strawberry (n = 22), decreasing concentrations in Na ($R^2 = 0.18$), Al ($R^2 = 0.54$), K ($R^2 = 0.21$), Ti ($R^2 = 0.43$), Fe ($R^2 = 0.51$, n = 21), Ni ($R^2 = 0.37$, n = 20), Cu ($R^2 = 0.31$, n = 21), Zn ($R^2 = 0.84$, n = 21), Sb ($R^2 = 0.41$, n = 22), and increasing concentrations in Cr ($R^2 = 0.39$, n = 20) were observed ($p < 0.05$).

The exposed leaves were investigated using both ED-XRF and HR-ICP-MS techniques for a total of ten (common) elements (Si, K, Ca, Ti, Cr, Fe, Cu, Rb, Sr, Pb), for which concentrations were always higher when measured by ED-XRF (Table 1) in comparison with the ICP-MS (Table 2) determination of the leaf washing solutions. However, those ten elements were detected for most analyzed leaves with ICP-MS, what was not the case for ED-XRF. For the latter, the number and frequency of detected elements was rather low, and in some cases only detected on the adaxial or on the abaxial leaf surface (*e.g.* Si, Ti, Cr) (Figure S.6). The contributions of each separate leaf side could not be distinguished for with ICP-MS, while with ED-XRF each leaf surface could be measured separately.

Whenever both leaf sides were quantifiable for the considered elements, the average of the two leaf concentrations was calculated to obtain leaf-level ED-XRF concentration values. Otherwise, either the adaxial or abaxial concentrations were used. As mentioned before, the complex matrix of plant leaves interferes with the operational and measuring principle of ED-XRF, leading to large between-sample variability. Therefore, we consider the accumulation of elements throughout this campaign to be most accurately represented by the concentrations quantified by HR-ICP-MS on the leaf washing solutions (Figure 2). Elements K and Ca can originate from crustal dust (Tomašević and Aničić, 2010; Vercauteren et al., 2011), as well as from foliar exchange and leaching in the form of cations (K^+ and Ca^{2+}). K^+ is a highly mobile plant electrolyte, while Ca^{2+} is bound to structural plant tissues or enzyme complexes (Draaijers et al., 1994; Kopáček et al., 2009). As they can easily be transferred into the washing solutions, high concentrations of both K and Ca are observed (Figure 2, center). Disregarding those components from the composition profile (Figure 2, rightmost), the relative contribution of anthropogenic, traffic-related metals is comparable between ivy and strawberry species, with Fe > Cu ≈ Pb > Cr. Yet, these relative contributions appear to be very different when compared to the obtained ED-XRF concentrations (Figure 2, leftmost).

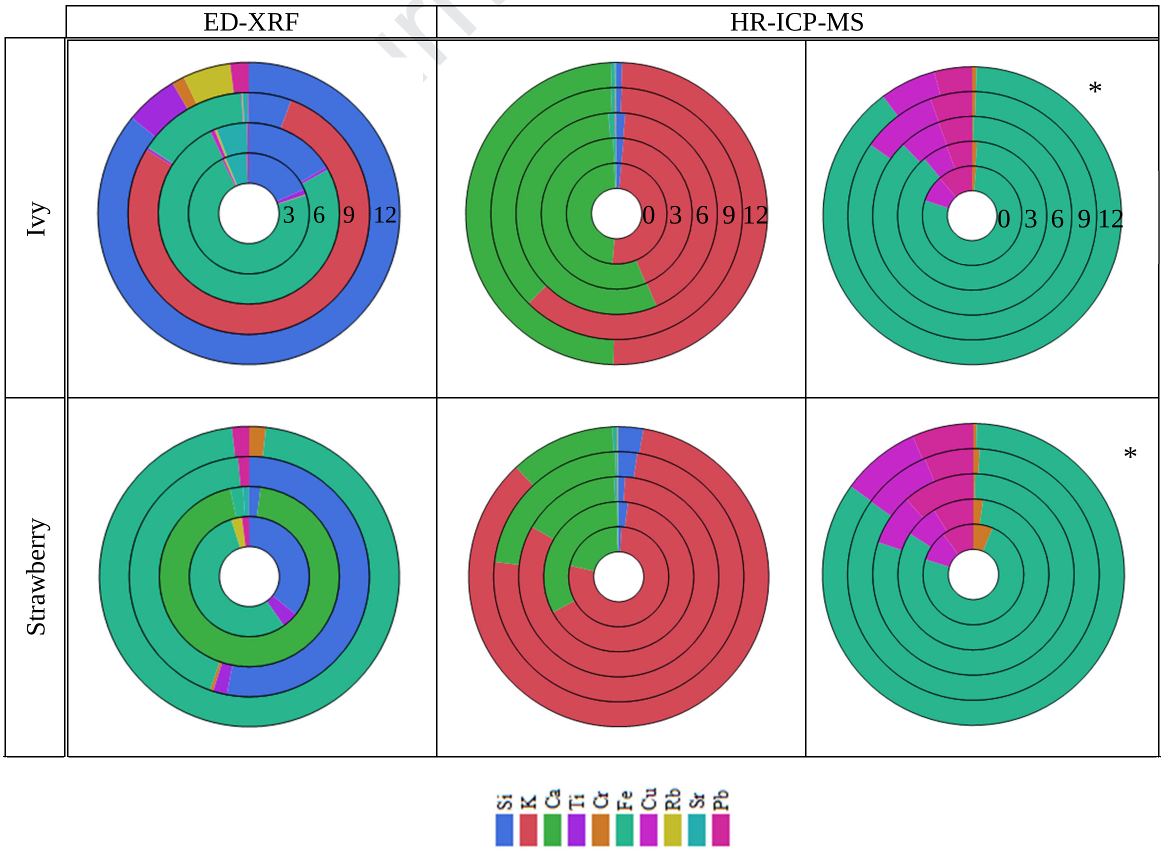

*Figure 2 – Pie charts of average leaf surface elemental concentrations (Si, K, Ca, Ti, Cr, Fe, Cu, Rb, Sr, Pb) measured by ED-XRF and HR-ICP-MS for ivy and strawberry leaves throughout the exposure campaign (0-3-6-9-12 weeks). The piecharts in the rightmost column (indicated with *) display only a selection of the traffic-related elements (Cr, Fe, Cu, Pb).*

The evolution of ED-XRF leaf concentrations over exposure time was not linear nor consistent among all investigated elements. However, leaf concentrations showed a relative decrease after six weeks of exposure with values growing again on 12w leaves for Si, Ti and Pb (Figure 3). The concentrations measured via ICP-MS on the leaf washing solutions did not show a consistent temporal pattern either (Figure 3). The concentrations in Ti, Cu and Pb were the highest for the 6w leaves, with values decreasing on 9w and then increasing for 12w leaves. On the other hand, such patterns were rather diverse for the remaining elements (Si, K, Ca, Cr, Fe, Cu, Rb, Sr) and also species-dependent. When comparing the leaves obtained at the end of the exposure campaign (12w) against the non-exposed leaves (0w), elemental concentrations of K (strawberry, $p = 0.016$), Ca (ivy, $p = 0.008$), Ti (ivy and strawberry, $p = 0.032$ and $p = 0.016$) and Fe (strawberry, $p = 0.036$) decreased significantly, suggesting a reduced contribution of crustal dust matter (K, Ca, Ti, Fe) (Vercauteren et al., 2011). In contrast, a significant enrichment in Cr, often linked to traffic and corrosion sources (especially under railway/subway influences, considered negligible at the test site though) (Gehrig et al., 2007), was displayed on both ivy and strawberry. An exploratory PCA on the surface elemental concentrations (determined by ICP-MS) throughout the exposure period (Figure 4) also suggests the contribution of Cr to be closely connected with the exposure time at the test site. The two most discriminant components, PC1 and PC2, accounted for 55.7% of the total variance in all sampled leaves. The element Cr and 'exposure' (negative PC1 values) are separated from the remaining elements (Figure 4, a)), and reflected in the gradient going from non-exposed to 12-weeks exposed leaves (Figure 4, b)). The PC2 allows the distinction between crustal dust and leaf-occurring elements (K, Rb, Sr; negative PC2 values) and anthropogenic dust (Fe, Cu, Pb, Cr; positive PC2 values). Comparable conclusions are obtained from analyzing the two plant species separately (Figure S.7), with the highest concentrations in traffic-derived elements (Fe, Cu, Pb, Cr) being clearly depicted by 6w and 12w leaves.

The test site, located in a residential area and close to the university campus, is considered to be subjected to moderate car traffic. However, the intensity of car traffic may have decreased gradually during our exposure campaign, particularly from the end of June onwards with the start of the summer holidays period. This ‘holiday effect’ is supported by the relatively lower particulate and gaseous atmospheric concentrations observed during the second half of July (Figure S.1), and further confirmed by the negative Spearman’s correlations ($p < 0.01$) between NO_2 ($\rho = -0.36$), PM_{10} ($\rho = -0.43$) and $PM_{2.5}$ ($\rho = -0.32$) concentrations with day of the year (DOY) during the campaign. Daily fluctuations of atmospheric pollutants were consistent over the entire exposure period ($p < 0.01$; $\rho = 0.90$ between PM_{10} and $PM_{2.5}$ concentrations, $\rho = 0.43$ and $\rho = 0.41$ between $PM_{2.5}$ and NO_2, and PM_{10} and NO_2, respectively) (Table S.7), suggesting road traffic (NO_x and PM) as main local contributing source (McIntosh et al., 2007).

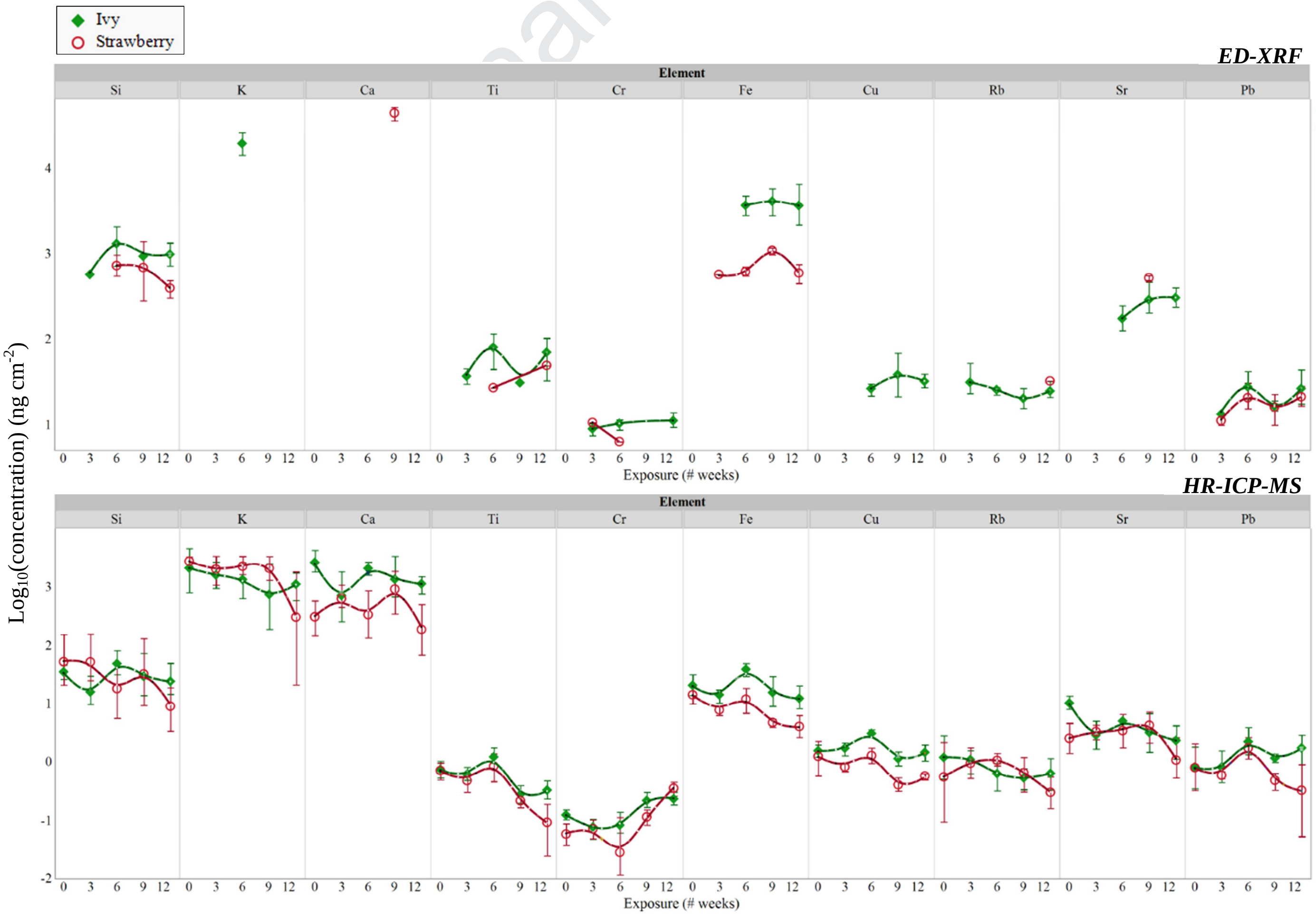

Figure 3 – Evolution of (log-transformed) elemental concentrations (Si, K, Ca, Ti, Cr, Fe, Cu, Rb, Sr, Pb) found for ivy (in green) and strawberry (in red) plant leaves throughout exposure time, as measured by ED-XRF (top) and HR-ICP-MS (bottom). Mean values are presented and the interval bars represent the interquartile ranges.

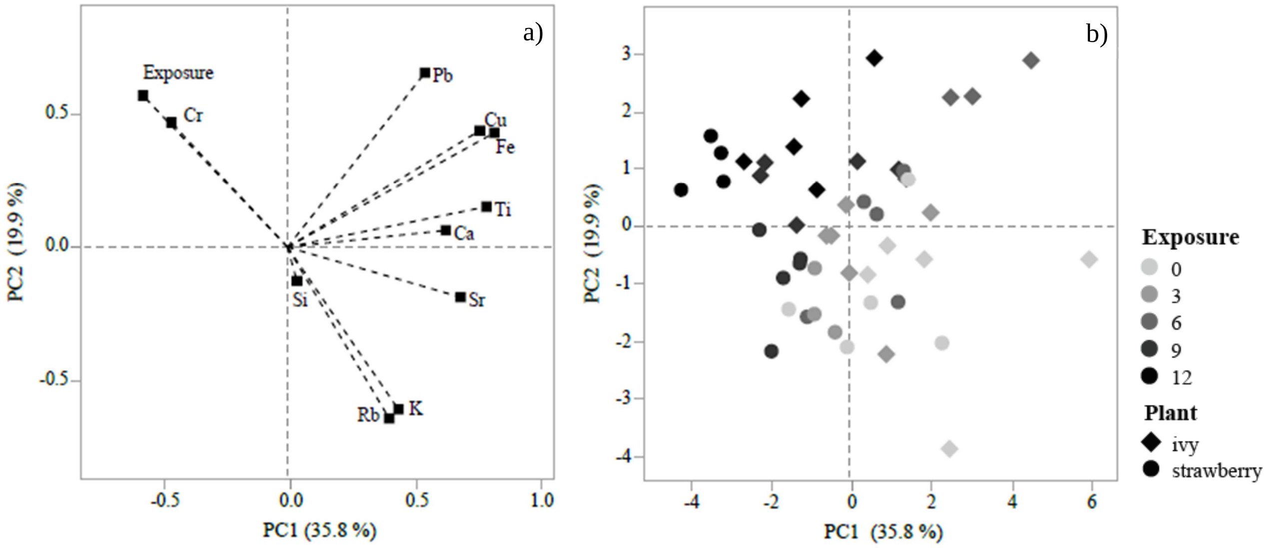

Figure 4 – Outputs of the PCA performed on the elemental concentrations measured by HR-ICP-MS on the leaf washing solutions, considering as input variables the 10 elements (Si, K, Ca, Ti, Cr, Fe, Cu, Rb, Sr, Pb) and the exposure time (in weeks). The projection in the PC1-PC2 plane of the a) input variables and b) analyzed samples, according to their plant species and exposure period, is shown, with PC1 and PC2 explaining 55.7% of the total variance. The same outputs were obtained separately for ivy and strawberry leaf samples and can be found in Figure S.7.

Table 1 - Mean leaf surface elemental concentrations (ng cm^{-2}) obtained via ED-XRF per plant species (ivy and strawberry), leaf side (adaxial and abaxial) and exposure time in weeks. Due to the reduced detection of elements, only the mean values (n = 1 to 6) are presented while standard deviations are not shown; "-" indicates that the element was not detected/quantified. Only the common elements (Si, K, Ca, Ti, Cr, Fe, Cu, Rb, Sr, Pb) are shown. Concentrations of other investigated elements and individual leaf concentrations can be found in the supplementary material (Tables S.2, S.4).

Plant	Leaf side	#Weeks	Si	K	Ca	Ti	Cr	Fe	Cu	Rb	Sr	Pb
Ivy	adaxial	3	567.1	-	-	37.4	8.6	-	-	33.3	-	13.1
		6	1462.9	14108.0	-	88.5	11.7	3497.9	29.8	25.1	126.3	30.0
		9	929.6	-	-	30.7	-	3683.0	45.0	18.9	268.7	14.9
		12	1025.9	-	-	78.7	11.2	4787.9	27.1	22.2	272.9	28.4
	abaxial	3	-	-	-	-	9.4	-	-	34.0	-	-
		6	-	25986.3	-	-	8.8	4060.0	24.2	26.0	218.5	30.5
		9	-	-	-	-	-	4944.4	-	22.5	358.8	17.6
		12	-	-	-	-	-	3659.5	34.9	27.9	370.2	29.5
Strawberry	adaxial	3	-	-	-	-	-	-	-	-	-	9.8
		6	757.9	-	-	-	-	-	-	-	-	22.4
		9	1667.6	-	51342.4	-	-	-	-	-	492.8	14.3
		12	495.2	-	-	49.0	-	614.5	-	32.2	-	22.1
	abaxial	3	-	-	-	-	10.5	568.7	-	-	-	12.3
		6	-	-	-	26.8	6.3	616.7	-	-	-	21.7
		9	411.3	-	40198.1	-	-	1090.6	-	-	543.9	21.4
		12	371.1	-	-	-	-	615.9	-	-	-	23.0

Table 2 - Mean and standard deviation (white and grey shading, respectively) of leaf elemental concentrations (ng cm^{-2}) obtained via HR-ICP-MS, per plant species (ivy and strawberry) and exposure time in weeks (n = 1 to 6); "-" indicates that the element was not detected/quantified. Only the common elements (Si, K, Ca, Ti, Cr, Fe, Cu, Rb, Sr, Pb) are shown. Concentrations of other investigated elements and individual leaf concentrations can be found in the supplementary material (Tables S.3, A.5).

Plant	#Weeks	Si	K	Ca	Ti	Cr	Fe	Cu	Rb	Sr	Pb
Ivy	0	36.64	3090.62	3044.93	0.78	0.13	23.44	1.60	1.59	10.74	1.08
		11.50	1977.39	2107.74	0.27	0.03	15.07	0.44	1.29	4.42	0.78
	3	19.40	1856.09	1109.86	0.65	0.08	15.00	1.75	1.22	3.36	0.97
		12.23	1183.67	993.10	0.28	0.03	6.02	0.41	0.58	1.94	0.63
	6	53.37	1638.76	2143.87	1.28	0.09	39.67	3.08	0.71	5.14	2.49
		29.24	1079.02	572.65	0.53	0.05	10.17	0.51	0.32	1.49	1.41
	9	50.89	1422.65	1871.07	0.29	0.22	18.53	1.17	0.59	4.02	1.18
		69.77	1248.29	1720.39	0.12	0.07	13.18	0.32	0.26	2.76	0.26
	12	39.37	1260.61	1209.33	0.35	0.24	13.90	1.52	0.73	2.83	2.01
		52.86	609.33	429.12	0.17	0.06	8.58	0.49	0.43	1.53	1.10
Strawberry	0	87.38	2827.98	374.10	0.74	0.06	14.94	1.50	1.20	3.13	1.16
		104.39	617.48	220.77	0.26	0.03	5.06	0.87	1.21	2.54	0.97
	3	72.37	2257.68	685.42	0.49	0.07	7.84	0.82	1.06	3.38	0.59
		73.48	1158.33	347.57	0.17	0.03	1.41	0.13	0.63	0.94	0.09
	6	30.14	2398.66	464.33	0.96	0.05	13.10	1.34	1.15	4.08	1.90
		31.23	911.87	377.97	0.48	0.06	5.85	0.44	0.59	2.51	0.93
	9	71.09	2360.93	1180.23	0.22	0.12	4.76	0.42	0.78	5.10	0.51
		95.19	1342.80	775.58	0.06	0.04	0.85	0.13	0.47	2.74	0.17
	12	11.20	951.70	254.80	0.13	0.36	4.29	0.58	0.36	1.34	0.60
		7.77	923.40	225.01	0.08	0.10	1.85	0.08	0.28	1.12	0.41
blanks		-	11.83	24.37	0.04	0.31	0.80	-	0.08	-	0.01
		-	11.04	-	0.04	-	0.62	-	0.06	-	-

3.3 Leaf magnetic analysis

Magnetic susceptibility of exposed leaves was almost negligible and often negative, with χ_{mass} values ranging from -6.5 to 4.4 $\times10^{-8}$ m^3 kg^{-1} for ivy, and from -12.1 to 21.4 $\times10^{-8}$ m^3 kg^{-1} for strawberry. Although values are comparable with results obtained in other leaf monitoring studies, *e.g.* from pine needles exposed for 3-8 months in Cologne, Germany (Lehndorff et al., 2006) or from leaves of *Platanus spp.*, *Quercus spp.*, *Tilia spp.*, *Nerium oleander* sampled monthly during 4-10 months in Northern Portugal (Sant'Ovaia et al., 2012), the k values measured in our study (range -3 to 4 $\times10^{-6}$ SI) are very close to the resolution of the measuring equipment (2×10^{-6} SI). This indicates that the concentration of magnetic particles accumulated over 3-months of exposure at the selected site was not sufficient to overcome the diamagnetic nature of the plant leaves, mainly composed of water and organic content. A similar observation was made for lime tree leaves collected at the end of the growing season in Lancaster, England (Mitchell and Maher, 2009). Rodríguez-Germade et al. (2014) have also reported negative and low χ_{mass} values for leaves of *Platanus hispanica* in the urban region of Madrid, Spain, yet with a more than thirty-fold increase (maximum of 32.2×10^{-8} m^3 kg^{-1}) after a total exposure of eight months. Such increasing trend over time was not evident in our data though (Table 3).

The application of various AC/DC combinations for leaf samples to acquire ARM (magnetic moment), showed that the largest intensity fields (AC 200mT and DC 500µT, $ARM_{200/500}$) led to the highest ARM values (Figure S.8). ARM depends on the mineralogy and concentration of magnetic particles, as well as on their magnetic grain size, with small single domain (SD) grains acquiring ARM more efficiently than multi domain (MD) grains (Liu et al., 2012b). Raw $ARM_{200/500}$ values were significantly larger for ivy than for strawberry ($p < 0.0001$), with exposed ivy (3w, 6w, 9w, 12w) and strawberry leaves (6w, 9w) exhibiting higher values compared to the non-exposed leaves (0w) ($p < 0.035$ and $p < 0.045$, respectively) (Figure S.9). For magnetic concentration indicators (χ_{mass}, SIRM, ARM), it is more useful to consider the values normalized for either mass or leaf surface area than the obtained magnetic moments. While mass-normalization is logical for assessing *e.g.* the amount and concentration of dust collected actively on pumped-air PM filters that have the same size, leaf monitoring is based on the fact that leaves accumulate PM passively on their surface. For the same plant species and equal exposure to pollutants, leaves with large surfaces accumulate more. For comparative purposes, results both normalized by mass and surface area are shown in Table 3. $ARM_{200/500}$ ranged between 0.24 µA and 1.09 µA for ivy and between 0.15 µA and 1.18 for strawberry species, being on average larger for ivy than for strawberry ($p < 0.0001$). For SIRM, one of the most investigated properties in the field of environmental magnetism, values ranged from 5.24 µA to 19.27 µA (Table 3). Ivy leaves accumulated higher concentrations of magnetic particles in comparison to strawberry ($p = 0.003$), with an average SIRM of 13.15 µA ± 3.57 µA (standard deviation) against 10.06 µA ± 4.18 µA, respectively. The obtained results are relatively low and comparable to values measured in parks or green areas, not reflecting the car traffic (although moderate and likely to have declined during the exposure campaign) in the nearby street road. In the province of Antwerp, passive monitoring studies using ivy from distinct land use types had shown a mean SIRM of 24 µA for a forested site compared to 205 µA for a busy roadside intersection with intense traffic (Castanheiro et al., 2016). In the same study area Smets et al. (2016) could magnetically recognize urban areas (mean SIRM of 200 µA) against green residential areas (mean of

31 µA). Similar outcomes were reported after a wide spatial study with 110 sampling locations in the city of Antwerp, in which the SIRM of ivy leaves was found to be correlated with traffic intensity (Hofman et al., 2014b). At a European-scale, leaf SIRM of *Platanus acerifolia* tree leaves collected at the end of their growing season revealed mean SIRM values of 30 µA and 153 µA for park and street sites, respectively. The minimum values of 7 µA (park site in Copenhagen, Denmark) and 9 µA (street site in Kavala, Greece) (Baldacchini et al., 2017) obtained in that study are in line with the values measured in our study.

The evolution of leaf SIRM throughout the exposure period was distinct for the two test species (Figure 5). Leaf SIRM of ivy increased significantly from three weeks onwards, as leaves from 6w, 9w and 12w had higher SIRM values than the non-exposed leaves ($p < 0.01$). For strawberry, an enrichment in magnetic grains was evident after three weeks of exposure as well, with the highest SIRM values obtained for 6w leaves ($p < 0.04$). However, this magnetic enrichment appeared to decrease after six weeks until the end of the exposure campaign. The latter results are unexpected as SIRM accumulation throughout the in-leaf season was found to be significant for 2-weekly collected Plane tree leaves in the same street of our monitored site, only affected at the end of the in-leaf season by leaf senescence (Hofman et al., 2014a). We hypothesize that the observed decrease may be due to the heavy rainfall after six weeks and that strawberry leaves are more sensitive to wash-off compared to ivy leaves. Furthermore, we noticed during leaf sampling that new leaves (both for ivy and strawberry) rapidly sprouted between the various sampling moments. This complicated the distinction between leaves exposed since the beginning of the campaign and newly emerged leaves, particularly at the end of the exposure period. This possible variation in exposure period may have influenced our results, as dust accumulation on the leaves was not so evident in terms of surface deposited elements nor magnetic enrichment, and a large variation was sometimes observed within the leaves sampled at the same moment. Leaf monitoring campaigns following this study were improved by labelling all plant leaves at the start of the exposure period. Nonetheless, meteorological conditions and the moderate road traffic, considered to decline at the second half of the exposure period, appear to be key factors in the leaf accumulation of dust at this test site. Such influences should not be overlooked as they are also relevant in terms of human exposure to atmospheric PM. Moreover, the test site is rather open, leading to ventilation effects, *i.e.* diluting the air pollutants (Janhäll, 2015).

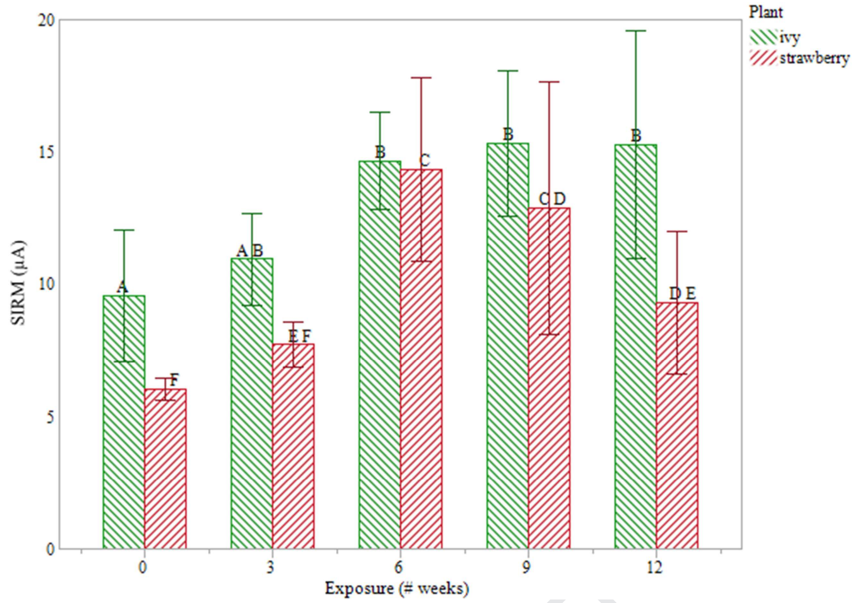

Figure 5 – Evolution of leaf SIRM for ivy (in green) and strawberry (in red) plant leaves throughout the exposure time in (weeks). Levels not associated with the same letter indicate (log-transformed) SIRM to be significantly different at p < 0.01 for ivy (A, B) and p < 0.04 for strawberry (C, D, E, F) leaves.

Obtained IRM_{-300} values were similar to SIRM values (Table 3), with subsequent S-ratio close to the unity (0.94 – 0.99 for ivy, 0.90 – 1.11 for strawberry), which indicates the remanence to be dominated by low-coercivity carriers such as magnetite-type minerals (Evans and Heller, 2003; Hansard et al., 2011; Hofman et al., 2017). Mean HIRM values varied throughout the exposure campaign between 0.09 – 0.33 µA and 0.06 – 0.40 µA for ivy and strawberry leaves, respectively. Such low HIRM values reflect that saturation is already achieved by 300 mT for most leaf samples, as corroborated by the S-ratio and obtained IRM acquisition curves (Table S.8, Figure S.10). The exposed leaves achieved ca. 22% and 69% of the total SIRM at 50 mT and 100 mT, respectively, with the remaining 30% to be acquired between 100 mT and 1 T. The contribution of anti-ferromagnetic grains (*e.g.* hematite) is negligible since only 3% of the total SIRM was reached above 300 mT (Evans and Heller, 2003). The S-ratio and HIRM, *i.e.* descriptors of the relative contribution of low- to high-coercivity components, were similar for both test species, as they were exposed to the same polluting conditions. ARM/SIRM can be used as a grain size indicator, with higher values representing more fine-grained (SD or pseudo-single domain, PSD) particles in contrast with MD grains (Evans and

Heller, 2003; Shi et al., 2014). The ratio ARM/SIRM (24.5 – 71.2 x10^{-3}), or equivalent ARMχ/SIRM (3.5 – 17.9 m A^{-1}), was statistically larger for ivy than for strawberry leaves ($p < 0.0001$), however, with values falling within the standard deviation ranges of each other (Figure S.11). Taking these uncertainties into account, the ranges of ARM/SIRM values are still comparable between ivy and strawberry, while also not largely changing throughout the exposure period. This reveals no change in magnetic grain size of the deposited PM at the monitored site. Therefore, the difference in leaf macro- and micro-morphological characteristics between ivy and strawberry appears not to have a grain size selective influence on the accumulation of atmospheric dust. Our values (S-ratio and ARM/SIRM) are comparable to the observations of Shi et al. (2014) and Wang et al. (2017) for daily PM filters, and suggest high contributions of small-grained SD/PSD magnetite particles within the accumulated atmospheric dust (Evans and Heller, 2003).

Table 3 – Mean (in grey), standard deviation (Std) and range (minimum: Min; maximum: Max) of measured leaf magnetic properties, per plant species (ivy and strawberry) and exposure time in weeks (n = 6). χ is normalized by leaf dry mass; $ARM_{200/500}$ and SIRM are normalized for both leaf dry mass (A m^2 kg^{-1}) and surface area (A).

Plant	#Weeks	χ x10^{-8} (m^3 kg^{-1})	$ARM_{200/500}$ x10^{-6} (A m^2 kg^{-1})	$ARM_{200/500}$ (µA)	ARMχ x10^{-8} (m^3 kg^{-1})	SIRM x10^{-6} (A m^2 kg^{-1})	SIRM (µA)	IRM_{-300} (µA)	HIRM (µA)	S-ratio (-)	ARM/SIRM x10^{-3} (-)	
Ivy	0	0.24	4.81	0.43	1.21	108.2	9.57	9.39	0.09	0.98	43.80	*Mean*
		3.90	1.68	0.15	0.42	27.5	2.51	2.45	0.05	0.01	7.55	*Std*
		-6.48	2.57	0.24	0.64	80.4	7.43	7.29	0.03	0.97	31.97	*Min*
		3.81	7.61	0.69	1.91	159.7	14.47	14.16	0.16	0.99	54.08	*Max*
	3	0.52	7.68	0.66	1.93	126.7	10.94	10.55	0.19	0.96	59.70	*Mean*
		2.82	2.97	0.15	0.74	39.8	1.75	1.67	0.05	0.01	6.99	*Std*
		-3.56	4.80	0.46	1.20	89.1	8.80	8.51	0.14	0.96	52.67	*Min*
		4.37	12.56	0.88	3.15	199.7	13.94	13.37	0.28	0.97	71.22	*Max*
	6	0.53	6.93	0.83	1.74	122.3	14.67	14.01	0.33	0.96	56.74	*Mean*
		1.40	1.50	0.10	0.38	26.1	1.86	1.75	0.10	0.01	2.42	*Std*
		-1.89	5.20	0.74	1.30	88.2	12.48	12.12	0.18	0.94	52.86	*Min*
		2.06	9.60	1.00	2.41	165.6	17.22	16.46	0.45	0.97	59.04	*Max*
	9	-0.88	7.90	0.75	1.98	173.5	15.32	14.79	0.26	0.97	49.44	*Mean*

		2.30	1.99	0.26	0.50	53.6	2.74	2.13	0.14	0.01	6.16	*Std*
		-3.78	5.30	0.30	1.33	111.2	12.44	12.06	0.16	0.95	24.46	*Min*
		2.73	11.09	0.99	2.78	241.9	18.90	18.22	0.47	0.98	66.12	*Max*
	12	-0.69	7.18	0.82	1.80	133.3	15.26	14.90	0.18	0.98	54.31	*Mean*
		1.45	2.07	0.22	0.52	42.6	4.30	4.12	0.13	0.01	2.83	*Std*
		-2.43	4.33	0.56	1.09	77.0	9.93	9.66	0.04	0.96	49.64	*Min*
		1.10	9.65	1.09	2.42	194.4	19.27	18.62	0.32	0.99	56.39	*Max*
Strawberry	0	4.53	1.82	0.13	0.46	83.2	6.03	5.88	0.08	0.98	20.62	*Mean*
		4.51	1.46	0.10	0.37	10.5	0.43	0.44	0.07	0.02	15.72	*Std*
		0.00	0.00	0.00	0.00	68.1	5.24	5.10	-0.03	0.95	0.00	*Min*
		12.12	3.60	0.23	0.90	99.3	6.39	6.45	0.15	1.01	38.19	*Max*
	3	-0.97	6.55	0.38	1.64	131.8	7.72	7.60	0.06	0.98	48.98	*Mean*
		11.67	2.40	0.10	0.60	31.5	0.86	1.32	0.27	0.06	8.02	*Std*
		-12.06	4.49	0.26	1.13	98.3	6.71	6.31	-0.48	0.94	38.70	*Min*
		21.39	10.87	0.56	2.72	176.6	9.05	10.01	0.20	1.11	61.53	*Max*
	6	-5.25	11.97	0.74	3.00	235.1	14.34	13.54	0.40	0.95	50.04	*Mean*
		4.80	3.76	0.28	0.94	45.9	3.46	3.21	0.24	0.02	7.13	*Std*
		-11.18	6.53	0.48	1.64	149.7	10.92	10.38	0.24	0.90	43.62	*Min*
		0.00	17.95	1.18	4.50	285.4	18.78	17.94	0.87	0.96	62.89	*Max*
	9	-0.34	8.75	0.48	2.19	267.1	12.88	12.47	0.21	0.97	34.29	*Mean*
		5.05	3.86	0.35	0.97	74.3	4.78	4.98	0.17	0.01	8.29	*Std*
		-8.07	5.13	0.15	1.29	176.2	9.22	9.00	0.10	0.95	14.12	*Min*
		5.32	15.59	1.11	3.91	363.5	22.22	21.20	0.51	0.98	50.05	*Max*
	12	-1.72	5.70	0.36	1.43	147.0	9.31	9.15	0.08	0.99	37.78	*Mean*
		3.37	2.30	0.15	0.58	41.5	2.69	2.47	0.15	0.05	5.39	*Std*
		-6.97	3.05	0.20	0.77	95.7	5.84	6.28	-0.22	0.96	29.51	*Min*
		2.14	9.21	0.61	2.31	203.3	13.41	13.05	0.18	1.08	45.32	*Max*

3.4 Leaf-surface particle deposition

The accumulation of atmospheric dust in our study has shown to be species- (ivy accumulated more than strawberry) and element-specific (temporal trends of deposited elements varied *per* element), rather than influenced by the buildup of pollutants, which was not as substantial as we would expect. Nevertheless, the accumulation of particles was corroborated by the SEM images (Figures 6, 7), with larger amounts of deposited particles found on ivy than on strawberry leaves and with 6w leaves showing the highest quantities. The size and shape of leaf-surface deposited particles is diverse, as reported before (Ottelé et al., 2010; Sgrigna et al., 2015; Song et al., 2015). The most striking information is related with the dust accumulation over time, with particle number increasing from the non-exposed to the 6w leaves. Subsequently, the number of deposited particles decreased after nine weeks (9w) and slightly increased again at the end of the campaign (12w). This temporal pattern was also verified in the concentration of some leaf-accumulated elements (Si, Ti and Pb, ED-XRF; Ti, Cu and Pb, HR-ICP-MS) and by the leaf SIRM of strawberry leaves. Particle removal processes (*e.g.* due to rain) as hypothesized earlier, therefore, seem to be confirmed.

Leaves with rough ridges and containing trichomes accumulate more PM than smooth leaf surfaces (Mo et al., 2015; Sæbø et al, 2012; Weerakkody et al., 2018). Despite strawberry leaves contain more trichomes and have a more rugged micro-topography than ivy (section 3.1), the ivy leaves in our study had higher SIRM (Figure 5) and displayed a larger quantity of deposited particles compared to strawberry (Figures 6, 7). In a recent study of Muhammad et al. (2019), a total of 96 plant species (mainly tree and shrub species) grown in a common garden, located at ca. 250 m from our test site, were studied to investigate the relation between leaf traits and particle accumulation measured by SIRM. Although the density of leaf trichomes was again confirmed as enhancing the accumulation of particles, some plant species with high trichome density but low leaf wettability showed reduced particle accumulation (*i.e.*, low SIRM) (Muhammad et al., 2019). Both ivy and strawberry leaves are considered to be hydrophilic (Walker et al., 2015). Yet, we hypothesize that strawberry leaves are less hydrophilic than ivy leaves (Figures S.2, S.3), which may prevent the deposition of particles (Bakker et al., 1999; Barima et al., 2016). A wind tunnel experiment also showed that the permeability of strawberry leaves, *i.e.* the ability to let pass an air-flow, is significantly lower compared to the permeability of ivy leaves (Koch et al., 2019), whereas Baker and Hunt (1986) described difficulties in penetrating the trichome arrangements of strawberry leaves with simulated rain. To clarify the remaining questions, future leaf monitoring campaigns should include controlled scenarios on rain exposure (*e.g.* plants protected/unprotected from rain) and leaf age (labeling to avoid sampling of newly emergent leaves).

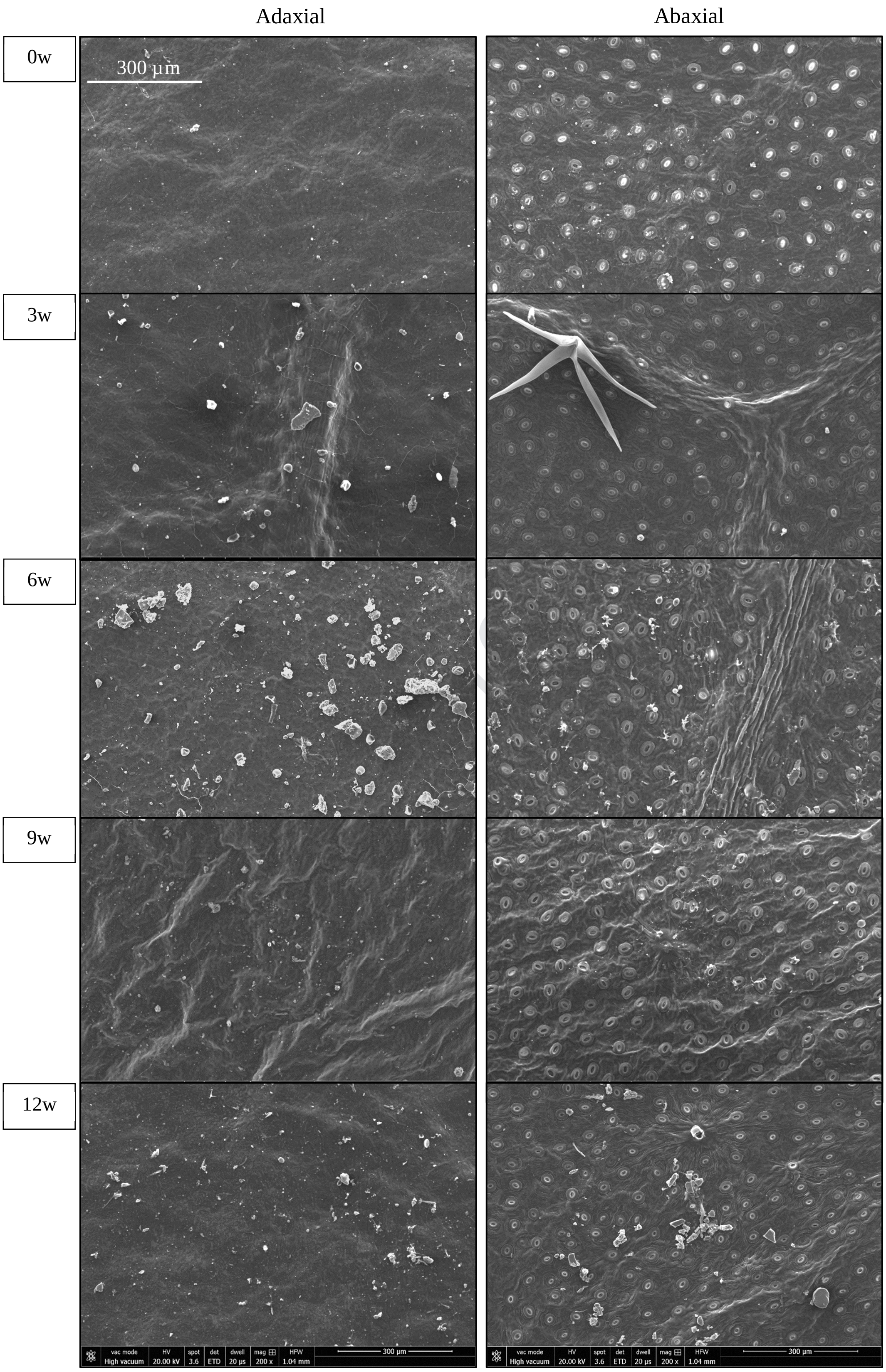

Figure 6 - Leaf surface SEM images from ivy leaves collected every three weeks (0w-3w-6w-9w-12w) throughout the total exposure period of three months. Both adaxial and abaxial leaf sides display leaf-deposited particles. A typical leaf trichome on ivy (of the stellate type (Ackerfield and Wen, 2002), is visible on image 3w-Abaxial. Magnification used is 200x, and the scale indicated in the upper left panel is similar for all panels.

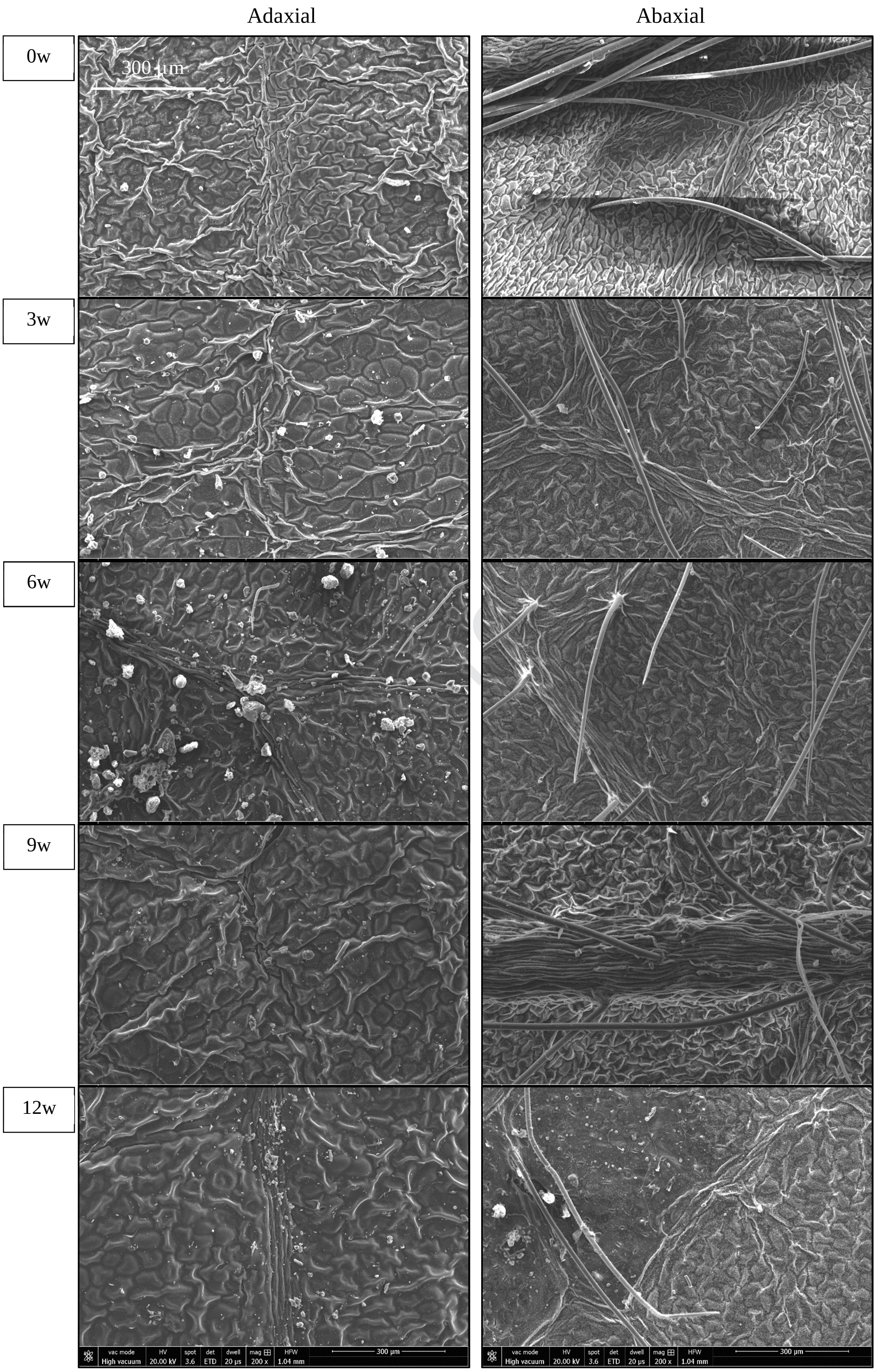

582 *Figure 7 - Leaf surface SEM images from strawberry leaves collected every three weeks (0w-3w-6w-9w-12w)*
583 *throughout the total exposure period of three months. Both adaxial and abaxial leaf sides display leaf-deposited*
584 *particles. Long trichomes are visible in all abaxial images. Magnification used is 200x, and the scale indicated*
585 *in the upper left panel is similar for all panels.*

3.5 Leaf accumulation of atmospheric dust - holistic analysis of a complex interaction

Due to the aforementioned reasons (low frequency of detection and large between-sample variability; section 3.2), concentrations of the accumulated elements were better assessed by analyzing the leaf leachates with ICP-MS than directly with ED-XRF. Reproducibility of the latter could be improved by grinding the leaf material, while sensitivity could be increased by *e.g.* combining selective excitation (through different secondary targets) with the reduction of the background of X-ray spectra (using polarized-beam instrumentation, PED-XRF) (Marguí et al., 2009).

For the elements measured by ICP-MS, trace metals such as Cr, Mn, Fe, Cu, Zn, and Pb, are of particular interest due to their potential hazardousness and link with anthropogenic pollution. With exception of Cr, which clearly built-up on the exposed leaves, the other metals have shown some fluctuation during the experiment (Figure S.12). Concentrations of Cu and Pb increased with exposure time until the 6w leaves (maximum values), after which they decreased slightly in a way that the overall enrichment at the end of the campaign is almost negligible. For other elements, however, the concentrations at the 0w leaves were the highest or equally high as for the 6w leaves, with values decreasing between 0w and 3w and increasing again between 3w and 6w. This is the case for Zn, Cu and Fe, which are known plant micronutrients (Gupta et al., 2009). We suspect that the enhanced concentrations in these metals at 0w are derived from the use of fertilizers or other treatments at the garden center, where the plants are kept attractive for people to acquire them. The low concentrations in Cr and Co at the 0w leaves support this argumentation, since they are not considered micronutrients. We hypothesize, thus, that between 0 and 3 weeks of exposure there is a natural depletion of Zn, Cu, and Fe due to decreasing fertilizer concentration. While traffic-related contributions start to accumulate on the leaves from the moment of exposure (Figures 6, 7), they do not overcome the natural, plant-internal contributions, and there is a decrease in total concentrations. Between 3 and 6 weeks, traffic contributions prevail and the elemental concentrations of Zn, Cu and Fe increase at 6w leaves. Between 6 and 12 weeks, these concentrations decrease again because of the rain (dust wash-off), the decrease in local atmospheric PM concentrations (particularly after 9w, leading to lower accumulation rates) and possibly the further natural depletion. In contrast to ICP-MS, the magnetic concentration indicators (ARM, SIRM) refer exclusively to traffic-related PM.

Regarding strawberries, ARM and SIRM were the smallest at 0w leaves, then increased until 6w and started to decrease until 12w (Figures 5, S.9). The same trend is observed for ivy until 6w, but then the magnetic enrichment remained constant as there was not much further accumulation. The fact that there is no decrease (in ARM or SIRM) for ivy could be related to the different leaf macro/micro morphology with respect to strawberry. Our study and previous studies on aerodynamics (Baker and Hunt, 1986; Koch et al., 2019) suggest strawberry leaves to be relatively slow accumulators of atmospheric dust. They also appear to be more susceptible to *e.g.* wash-off effects and/or variation in PM contributions compared to ivy leaves, as the elemental and magnetic depletion after 6w occurred much rapidly for strawberry than for ivy. In order to estimate the degree of natural depletion of micronutrients, a blank plant growing in the laboratory should be monitored along with the plants exposed to pollution. This side process may be of even more relevance for monitoring low-polluted sites. Lastly, the difference in dust accumulation between ivy and strawberry might be related with the degree and/or rate of encapsulation of deposited particles, which become thus unsusceptible to wash-off. The influence of precipitation on the exposed leaves was difficult to evaluate because the leaves exposed for longer periods (thus, expected to accumulate more dust) were also subjected to total larger rain volumes. Studies on the leaf wettability of ivy and strawberry leaves, as well as on the dynamics of leaf encapsulation of particles (in addition to the deposition) could be of relevance to disentangle the observed species-specific accumulation patterns.

The elemental concentrations on the exposed leaves (ICP-MS) were for some elements (Cr, Co, Mn, Fe, Zn) correlated with the cumulative atmospheric pollutants (PM_{10}, $PM_{2.5}$) at the test site (Tables S.9, S.10; Figure S.13). For both ivy and strawberry, Cr was positively correlated with cumulative PM_{10} and $PM_{2.5}$, whereas Zn was negatively correlated. When relating the cumulative PM with the measured leaf magnetic properties, the indicators $ARM_{200/500}$, SIRM and ARMχ were positively correlated for ivy, and SIRM and ARMχ for strawberry (Tables S.11, S.12; Figure S.14). The average trace elements concentrations and magnetic indicators were compared for the five sampling events (0w, 3w, 6w, 9w, 12w). Significant correlations ($p = 0.038$; $\rho = 0.9$) were found for ivy only, between $ARM_{200/500}$ and the metals Co and Pb, and between SIRM and Mn. Further research should include performing these analyses (ICP-MS and magnetic) on the same leaves, to properly investigate the relationships between leaf magnetic properties and enrichment in trace elements, in terms of dust-polluting contributions and natural depletion.

4. Conclusions

In the present study ivy and strawberry plants were exposed outdoors at a moderate road traffic site for a period of three months. Leaves collected every three weeks were analyzed for their elemental and magnetic content, as well as microscopically, in order to evaluate the accumulated leaf dust. Dust accumulation was mainly observed visually (SEM) and magnetically, on both ivy and strawberry leaves, while the enrichment in metals was limited (only Cr increased over time for both species). Dust wash-off effects due to rain and lowered atmospheric PM concentrations, between 6w and 12w, were reflected in the obtained results (mainly magnetically and via SEM images). The overall dust accumulation was not as substantial as expected, possibly due to the aforementioned reasons, and to the fact that traffic-related contributions were moderate. Yet, significant differences were observed between the two test species. Ivy accumulated more dust (elements/magnetically/SEM) than strawberry leaves, even though strawberry leaves are characterized by the presence of long trichomes and a rugged micromorphology, which are considered important leaf traits to capture atmospheric dust. In addition to accumulating less, strawberry leaves also seemed to be more susceptible to wash-off effects. The magnetic enrichment of exposed ivy and strawberry leaves was, nonetheless, equally derived from small-grained SD/PSD magnetite particles. The results from this campaign support ivy leaves to be useful and reliable in the monitoring of atmospheric dust, having also the advantage of being a resilient, evergreen species, widely available in a variety of environments, from natural to urban settings.

Leaf surface elemental concentrations were obtained from the same leaf samples with ED-XRF and HR-ICP-MS. Although ED-XRF requires no sample preparation and is reliable for the analysis of PM-filters, the observed blank variability was too high to get reliable quantifications, related with the fact that the leaf matrix is rather heterogeneous, chemically and in terms of thickness. The high frequency and consistency of elements detected by HR-ICP-MS in the leaf leachates supports this methodology as a useful approach to investigate the accumulation of atmospheric dust on leaf surfaces. By comparing the ICP-MS concentrations with the magnetic properties for the non-exposed leaves, there was evidence that certain elements (Cu, Fe, Zn) associated with traffic-related pollution might have been derived from the plants *per se* through the use of fertilizers (plant micronutrients). Plant leaves are valuable for monitoring the surrounding habitat quality. The present exposure campaign illustrated how complex and multifaceted the interaction between atmospheric dust and its accumulation on leaves can be. Variations in terms of pollution contributions, meteorological phenomena, species-specific traits, particle deposition (and encapsulation) *versus* micronutrients depletion, will normally have a different outcome depending on *e.g.* the polluting source/level, monitoring period and species used. Although not being completely elucidative, such multifactorial leaf dust accumulation process can better be understood through a combination of techniques (elements/magnetic/SEM).

5. Acknowledgements

The authors thank the Flemish Environment Agency (VMM) for their collaboration and air quality and meteorological data, and Karen Wuyts for the discussion about plant leaf characteristics. A.C. gratefully acknowledges the Research Foundation Flanders (FWO) for her PhD fellowship (1S21418N). J.H. received a FWO postdoctoral fellowship grant (12I4816N).

6. References

Ackerfield, J., Wen, J., 2002. A morphometric analysis of *Hedera L.* (the ivy genus, Araliaceae) and its taxonomic implications. Adansonia ser. 3 24, 197–212.

Alfani, A., Bartoli, G., Rutigliano, F.A., Maisto, G., Virzo De Santo, A., 1996. Trace metal biomonitoring in the soil and the leaves of *Quercus ilex* in the urban area of Naples. Biol. Trace Elem. Res. 51, 117–131. doi:10.1007/BF02790154

Amato, F., Pandolfi, M., Moreno, T., Furger, M., Pey, J., Alastuey, a., Bukowiecki, N., Prevot, A.S.H., Baltensperger, U., Querol, X., 2011. Sources and variability of inhalable road dust particles in three European cities. Atmos. Environ. 45, 6777–6787. doi:10.1016/j.atmosenv.2011.06.003

Amato, F., Schaap, M., Denier van der Gon, H.A.C., Pandolfi, M., Alastuey, A., Keuken, M., Querol, X., 2013. Short-term variability of mineral dust, metals and carbon emission from road dust resuspension. Atmos. Environ. 74, 134–140. doi:10.1016/j.atmosenv.2013.03.037

Baker, E.A., Hunt, G.M., 1986. Erosion of waxes from leaf surfaces by simulated rain. New Phytol. 102, 161–173. doi:10.1111/j.1469-8137.1986.tb00807.x

Bakker, M.I., Vorenhout, M., Sijm, D.T.H.M., Kollöffel, C., 1999. Dry deposition of atmospheric polycyclic aromatic hydrocarbons in three Plantago species. Environ. Toxicol. Chem. 18, 2289–2294. doi:10.1002/etc.5620181025

Baldacchini, C., Castanheiro, A., Maghakyan, N., Sgrigna, G., Verhelst, J., Alonso, R., Amorim, J.H., Bellan, P., Bojović, D., Breuste, J., Bühler, O., Cântar, I.C., Cariñanos, P., Carriero, G., Churkina, G., Dinca, L., Esposito, R., Gawroński, S.W., Kern, M., Le Thiec, D., Moretti, M., Ningal, T., Rantzoudi, E.C., Sinjur, I., Stojanova, B., Aničić Urošević, M., Velikova, V., Živojinović, I., Sahakyan, L., Calfapietra, C., Samson, R., 2017. How does the amount and composition of PM deposited on *Platanus acerifolia* leaves change across different cities in Europe? Environ. Sci. Technol. 51, 1147–1156. doi:10.1021/acs.est.6b04052

Barima, Y.S.S., Angaman, D.M., N'gouran, K.P., Koffi, N.A., Tra Bi, F.Z., Samson, R., 2016. Involvement of leaf characteristics and wettability in retaining air particulate matter from tropical plant species. Environ. Eng. Res. doi:10.4491/eer.2015.120

Barthlott, W., Neinhuis, C., Cutler, D., Ditsch, F., Meusel, I., Theisen, I., Wilhelmi., H., 1998. Classification and terminology of plant epicuticular waxes. Bot. J. Linn. Soc. doi:10.1006/bojl.1997.0137

Beckett, K.P., Freer-Smith, P.H., Taylor, G., 2000. Particulate pollution capture by urban trees: Effect of species and windspeed. Glob. Chang. Biol. 6, 995–1003. doi:10.1046/j.1365-2486.2000.00376.x

Bilo, F., Borgese, L., Dalipi, R., Zacco, A., Federici, S., Masperi, M., Leonesio, P., Bontempi, E., Depero, L., 2017. Elemental analysis of tree leaves by total reflection X-ray fluorescence: New approaches for air quality monitoring. Chemosphere 178, 504–512. doi:10.1016/j.chemosphere.2017.03.090

Breysse, P.N., Delfino, R.J., Dominici, F., Elder, A.C.P., Frampton, M.W., Froines, J.R., Geyh, A.S., Godleski, J.J., Gold, D.R., Hopke, P.K., Koutrakis, P., Li, N., Oberdörster, G., Pinkerton, K.E., Samet, J.M., Utell, M.J., Wexler, A.S., 2013. US EPA particulate matter research centers: Summary of research results for 2005-2011. Air Qual. Atmos. Heal. doi:10.1007/s11869-012-0181-8

Castanheiro, A., Samson, R., De Wael, K., 2016. Magnetic- and particle-based techniques to investigate metal deposition on urban green. Sci. Total Environ. 571, 594–602. doi:10.1016/j.scitotenv.2016.07.026

Chen, L., Liu, C., Zhang, L., Zou, R., Zhang, Z., 2017. Variation in tree species ability to capture and retain airborne fine particulate matter (PM2.5). Sci. Rep. 7, 3206. doi:10.1038/s41598-017-03360-1

De Nicola, F., Maisto, G., Prati, M.V.V., Alfani, A., 2008. Leaf accumulation of trace elements and polycyclic aromatic hydrocarbons (PAHs) in *Quercus ilex L.* Environ. Pollut. 153, 376–383. doi:10.1016/j.envpol.2007.08.008

De Nicola, F., Murena, F., Costagliola, M.A., Alfani, A., Baldantoni, D., Prati, M.V., Sessa, L., Spagnuolo, V., Giordano, S., 2013. A multi-approach monitoring of particulate matter, metals and PAHs in an urban street canyon. Environ. Sci. Pollut. Res. 20, 4969–4979. doi:10.1007/s11356-012-1456-1

Dockery, D., Pope, A., 1994. Acute respiratory effects of particulate air pollution. Annu. Rev. Public Health 15, 107–132. doi:10.1146/annurev.pu.15.050194.000543

Draaijers, G.P.J., Erisman, J.W., van Leeuwen, N.F.M., Römer, F.G., te Winkel, B.H., Vermeulen, A.T., Wyers, G.P., Hansen, K., 1994. A comparison of methods to estimate canopy exchange at the Speulder Forest. National Institute of Public Health and Environmental Protection, Bilthoven, The Netherlands. Report No. 722108004.

Dzierżanowski, K., Popek, R., Gawronska, H., Sæbø, A., Gawroński, S.W., 2011. Deposition of particulate matter of different size fractions on leaf surfaces and in waxes of urban forest species. Int. J. Phytoremediation 13, 1037–1046. doi:10.1080/15226514.2011.552929

EEA, 2017a. Emissions of the main air pollutants in Europe. https://www.eea.europa.eu/data-and-maps/indicators/main-anthropogenic-airpollutant-emissions/assessment-5. Accessed 28 September 2018.

EEA, 2017b. Exceedance of air quality standards in urban areas. https://www.eea.europa.eu/data-and-maps/indicators/exceedance-of-air-qualitylimit-3/assessment-3. Accessed 28 September 2018.

Evans, M.E., Heller, F., 2003. Environmental magnetism: Principles and applications of enviromagnetics. Geophys. Ser. 86, 1–299 (ISBN: 978–0–12-243851-6).

Galvão, E.S., Santos, J.M., Lima, A.T., Reis, N.C., Orlando, M.T.D., Stuetz, R.M., 2018. Trends in analytical techniques applied to particulate matter characterization: A critical review of fundaments and applications. Chemosphere. doi:10.1016/j.chemosphere.2018.02.034

Gehrig, R., Hill, M., Lienemann, P., Zwicky, C.N., Bukowiecki, N., Weingartner, E., Baltensperger, U., Buchmann, B., 2007. Contribution of railway traffic to local PM10 concentrations in Switzerland. Atmos. Environ. 41, 923–933. doi:10.1016/j.atmosenv.2006.09.021

Grote, R., Samson, R., Alonso, R., Amorim, J.H., Cariñanos, P., Churkina, G., Fares, S., Thiec, D. Le, Niinemets, Ü., Mikkelsen, T.N., Paoletti, E., Tiwary, A., Calfapietra, C., 2016. Functional traits of urban trees: air pollution mitigation potential. Front. Ecol. Environ. 14, 543–550. doi:10.1002/fee.1426

Gupta, U.C., Wu, K., Liang, S., 2008. Micronutrients in soils, crops, and livestock. Earth Sci. Front. 15, 110–125. doi:10.1016/S1872-5791(09)60003-8

Hansard, R., Maher, B.A., Kinnersley, R., 2011. Biomagnetic monitoring of industry-derived particulate pollution. Environ. Pollut. 159, 1673–1681. doi:10.1016/j.envpol.2011.02.039

Harrison, R.M., Yin, J., 2000. Particulate matter in the atmosphere: Which particle properties are important for its effects on health? Sci. Total Environ. 249, 85–101. doi:10.1016/S0048-9697(99)00513-6

Hobbie, S.E., Reich, P.B., Oleksyn, J., Ogdahl, M., Zytkowiak, R., Hale, C., Karolewski, P., 2006. Tree species effects on decomposition and forest floor dynamics in a common garden. Ecology 87, 2288–97.

Hofman, J., Lefebvre, W., Janssen, S., Nackaerts, R., Nuyts, S., Mattheyses, L., Samson, R., 2014b. Increasing the spatial resolution of air quality assessments in urban areas: A comparison of biomagnetic monitoring and urban scale modelling. Atmos. Environ. 92, 130–140. doi:10.1016/j.atmosenv.2014.04.013

Hofman, J., Maher, B.A., Muxworthy, A.R., Wuyts, K., Castanheiro, A., Samson, R., 2017. Biomagnetic monitoring of atmospheric pollution: A review of magnetic signatures from biological sensors. Environ. Sci. Technol. 51, 6648–6664. doi:10.1021/acs.est.7b00832

Hofman, J., Wuyts, K., Van Wittenberghe, S., Samson, R., 2014a. On the temporal variation of leaf magnetic parameters: Seasonal accumulation of leaf-deposited and leaf-encapsulated particles of a roadside tree crown. Sci. Total Environ. 493, 766–772. doi:10.1016/j.scitotenv.2014.06.074

Janhäll, S., 2015. Review on urban vegetation and particle air pollution – Deposition and dispersion. Atmos. Environ. 105, 130–137. doi:10.1016/j.atmosenv.2015.01.052

Jayamurugan, R., Kumaravel, B., Palanivelraja, S., Chockalingam, M.P., 2013. Influence of temperature, Relative humidity and seasonal variability on ambient air quality in a coastal urban area. Int. J. Atmos. Sci. 2013, 1–7. doi:10.1155/2013/264046

Kardel, F., Wuyts, K., De Wael, K., Samson, R., 2018. Biomonitoring of atmospheric particulate pollution via chemical composition and magnetic properties of roadside tree leaves. Environ. Sci. Pollut. Res. 25, 25994–26004. doi: 10.1007/s11356-018-2592-z

Kardel, F., Wuyts, K., Maher, B.A., Hansard, R., Samson, R., 2011. Leaf saturation isothermal remanent magnetization (SIRM) as a proxy for particulate matter monitoring: Inter-species differences and in-season variation. Atmos. Environ. 45, 5164–5171. doi:10.1016/j.atmosenv.2011.06.025

Kgabi, N.A., Mokgwetsi, T., 2009. Dilution and dispersion of inhalable particulate matter, in: WIT Transactions on Ecology and the Environment. WIT Press, pp. 229–238. doi:10.2495/RAV090201

Kim, K.W., Ahn, J.J., Lee, J.H., 2009. Micromorphology of epicuticular wax structures of the garden strawberry leaves by electron microscopy: Syntopism and polymorphism. Micron, 40(3), 327–334. doi: 10.1016/j.micron.2008.11.002

Koch, K., Samson, R., Denys, S., 2019. Aerodynamic characterisation of green wall vegetation based on plant morphology: An experimental and computational fluid dynamics approach. Biosyst. Eng. 178, 34–51. doi:10.1016/j.biosystemseng.2018.10.019

Kopáček, J., Turek, J., Hejzlar, J., Šantrůčková, H., 2009. Canopy leaching of nutrients and metals in a mountain spruce forest. Atmos. Environ. doi:10.1016/j.atmosenv.2009.07.031

Künzli, N., Kaiser, R., Medina, S., Studnicka, M., Chanel, O., Filliger, P., Herry, M., Horak, F., Puybonnieux-Texier, V., Quénel, P., Schneider, J., Seethaler, R., Vergnaud, J.C., Sommer, H., 2000. Public-health impact of outdoor and traffic-related air pollution: A European assessment. Lancet 356, 795–801. doi:10.1016/S0140-6736(00)02653-2

Laden, F., Neas, L.M., Dockery, D.W., Schwartz, J., 2000. Association of fine particulate matter from different sources with daily mortality in six U.S. cities. Environ. Health Perspect. 108, 941–947. doi:10.1289/ehp.00108941

Lammel, G., Röhrl, A., Schreiber, H., 2002. Atmospheric lead and bromine in Germany: Post-abatement levels, variabilities and trends. Environ. Sci. Pollut. Res. 9, 397–404. doi:10.1007/BF02987589

Lehndorff, E., Urbat, M., Schwark, L., 2006. Accumulation histories of magnetic particles on pine needles as function of air quality. Atmos. Environ. 40, 7082–7096. doi:10.1016/j.atmosenv.2006.06.008

Litschke, T., Kuttler, W., 2008. On the reduction of urban particle concentration by vegetation a review. Meteorol. Zeitschrift 17, 229–240. doi:10.1127/0941-2948/2008/0284

Liu, L., Guan, D., Peart, M.R., 2012a. The morphological structure of leaves and the dust-retaining capability of afforested plants in urban Guangzhou, South China. Environ. Sci. Pollut. Res. 19, 3440–3449. doi:10.1007/s11356-012-0876-2

Liu, Q., Roberts, A.P., Larrasoaa, J.C., Banerjee, S.K., Guyodo, Y., Tauxe, L., Oldfield, F., 2012b. Environmental magnetism: Principles and applications. Rev. Geophys. 50, RG4002. doi:10.1029/2012RG000393

Maher, B.A., Moore, C., Matzka, J., 2008. Spatial variation in vehicle-derived metal pollution identified by magnetic and elemental analysis of roadside tree leaves. Atmos. Environ. 42, 364–373. doi:10.1016/j.atmosenv.2007.09.013

Marguí, E., Hidalgo, M., Queralt, I., 2005. Multielemental fast analysis of vegetation samples by wavelength dispersive X-ray fluorescence spectrometry: Possibilities and drawbacks. Spectrochim. Acta - Part B At. Spectrosc. 60, 1363–1372. doi:10.1016/j.sab.2005.08.004

Marguí, E., Queralt, I., Hidalgo, M., 2009. Application of X-ray fluorescence spectrometry to determination and quantitation of metals in vegetal material. TrAC Trends Anal. Chem. 28, 362–372. doi:10.1016/J.TRAC.2008.11.011

Matzka, J., Maher, B.A., 1999. Magnetic biomonitoring of roadside tree leaves: identification of spatial and temporal variations in vehicle-derived particulates. Atmos. Environ. 33, 4565–4569. doi:10.1016/S1352-2310(99)00229-0

McIntosh, G., Gómez-Paccard, M., Osete, M.L., 2007. The magnetic properties of particles deposited on *Platanus x hispanica* leaves in Madrid, Spain, and their temporal and spatial variations. Sci. Total Environ. 382, 135–146. doi:10.1016/j.scitotenv.2007.03.020

Mitchell, R., Maher, B.A., 2009. Evaluation and application of biomagnetic monitoring of traffic-derived particulate pollution. Atmos. Environ. 43, 2095–2103. doi: 10.1016/j.atmosenv.2009.01.042

Mo, L., Ma, Z., Xu, Y., Sun, F., Lun, X., Liu, X., Chen, J., Yu, X., 2015. Assessing the capacity of plant species to accumulate particulate matter in Beijing, China. PLoS One 10, e0140664. doi:10.1371/journal.pone.0140664

Moretti, S., Smets, W., Hofman, J., Mubiana, K.V., Oerlemans, E., Vandenheuvel, D., Samson, R., Blust, R., Lebeer, S., 2019. Human inflammatory response of endotoxin affected by particulate matter-bound transition metals. Environ. Pollut. 244, 118–126. doi: 10.1016/J.ENVPOL.2018.09.148

Muhammad, S., Wuyts, K., Samson, R., 2019. Atmospheric net particle accumulation on 96 plant species with contrasting morphological and anatomical leaf characteristics in a common garden experiment. Atmos. Environ. 202, 328–344. doi:10.1016/j.atmosenv.2019.01.015

Okuda, T., Fujimori, E., Hatoya, K., Takada, H., Kumata, H., Nakajima, F., Hatakeyama, S., Uchida, M., Tanaka, S., He, K., Ma, Y., Haraguchi, H., 2013. Rapid and simple determination of multi-elements in aerosol samples collected on quartz fiber filters by using EDXRF coupled with fundamental parameter quantification technique. Aerosol Air Qual. Res. 13, 1864–1876. doi:10.4209/aaqr.2012.11.0308

Ottelé, M., van Bohemen, H.D., Fraaij, A.L.A., 2010. Quantifying the deposition of particulate matter on climber vegetation on living walls. Ecol. Eng. 36, 154–162. doi:10.1016/j.ecoleng.2009.02.007

Poorter, H., Niinemets, Ü., Poorter, L., Wright, I.J., Villar, R., 2009. Causes and consequences of variation in leaf mass per area (LMA): a meta-analysis. New Phytol. 182, 565–588. doi:10.1111/j.1469-8137.2009.02830.x

Pope, A., Burnett, R.T., Thun, M.J., Calle, E.E., Krewski, D., Ito, K., Thurston, G.D., Thurston, G.D., 2002. Lung cancer, cardiopulmonary mortality, and long-term exposure to fine particulate air pollution. JAMA 287, 1132–41. doi:10.1001/jama.287.9.1132

Popek, R., Gawrońska, H., Wrochna, M., Gawroński, S.W., Sæbø, A., 2013. Particulate matter on foliage of 13 woody species: deposition on surfaces and phytostabilisation in waxes - a 3-Year Study. Int. J. Phytoremediation 15, 245–256. doi:10.1080/15226514.2012.694498

Przybysz, A., Sæbø, A., Hanslin, H.M., Gawroński, S.W., 2014. Accumulation of particulate matter and trace elements on vegetation as affected by pollution level, rainfall and the passage of time. Sci. Total Environ. 481, 360–369. doi:10.1016/j.scitotenv.2014.02.072

Rodríguez-Germade, I., Mohamed, K., Rey, D., Rubio, B., García, A., 2014. The influence of weather and climate on the reliability of magnetic properties of tree leaves as proxies for air pollution monitoring. Sci. Total Environ. 468–469, 892–902. doi:10.1016/j.scitotenv.2013.09.009

Sæbø, A., Popek, R., Nawrot, B., Hanslin, H.M., Gawronska, H., Gawroński, S.W., 2012. Plant species differences in particulate matter accumulation on leaf surfaces. Sci. Total Environ. 427–428, 347–354. doi:10.1016/j.scitotenv.2012.03.084

Sant'Ovaia, H., Lacerda, M.J., Gomes, C.R., 2012. Particle pollution - An environmental magnetism study using biocollectors located in northern Portugal. Atmos. Environ. 61, 340–349. doi:10.1016/j.atmosenv.2012.07.059

Sawidis, T., Breuste, J., Mitrovic, M., Pavlovic, P., Tsigaridas, K., 2011. Trees as bioindicator of heavy metal pollution in three European cities. Environ. Pollut. 159, 3560–70. doi:10.1016/j.envpol.2011.08.008

Schwarze, P.E., Øvrevik, J., Låg, M., Refsnes, M., Nafstad, P., Hetland, R.B., Dybing, E., 2006. Particulate matter properties and health effects: Consistency of epidemiological and toxicological studies. Hum. Exp. Toxicol. doi:10.1177/096032706072520

Sgrigna, G., Sæbø, A., Gawroński, S.W., Popek, R., Calfapietra, C., 2015. Particulate Matter deposition on *Quercus ilex* leaves in an industrial city of central Italy. Environ. Pollut. 197, 187–194. doi:10.1016/j.envpol.2014.11.030

Shi, M., Wu, H., Zhang, S., Li, H., Yang, T., Liu, W., Liu, H., 2014. Weekly cycle of magnetic characteristics of the daily PM2.5 and PM2.5–10 in Beijing, China. Atmos. Environ. 98, 357–367. doi:10.1016/J.ATMOSENV.2014.08.079

Smets, W., Wuyts, K., Oerlemans, E., Wuyts, S., Denys, S., Samson, R., Lebeer, S., 2016. Impact of urban land use on the bacterial phyllosphere of ivy (*Hedera sp.*). Atmos. Environ. 147, 376–383. doi:10.1016/j.atmosenv.2016.10.017

Song, Y., Maher, B.A., Li, F., Wang, X., Sun, X., Zhang, H., 2015. Particulate matter deposited on leaf of five evergreen species in Beijing, China: Source identification and size distribution. Atmos. Environ. 105, 53–60. doi:10.1016/j.atmosenv.2015.01.032

Thompson, R., Oldfield, F., 1986. Environmental magnetism. Allen and Unwin, London, 227pp.

Tomašević, M., Aničić Urošević, M., 2010. Trace element content in urban tree leaves and SEM-EDAX characterization of deposited particles. Facta Univ. - Ser. Physics, Chem. Technol. 8, 1–13. doi:10.2298/FUPCT1001001T

Tomašević, M., Vukmirović, Z., Rajšić, S., Tasić, M., Stevanović, B., 2005. Characterization of trace metal particles deposited on some deciduous tree leaves in an urban area. Chemosphere 61, 753–760. doi:10.1016/j.chemosphere.2005.03.077

UNECE, 2012. Decision 2012/2, Amendment of the text of and annexes II to IX to the 1999 Protocol to Abate Acidification, Eutrophication and Ground-level Ozone and the addition of new annexes X and XI (http://www.unece. org/fileadmin/DAM/env/lrtap/full text/ECE_EB.AIR_111_ Add1_2_E.pdf). Accessed 28 September 2018.

Vercauteren, J., Matheeussen, C., Wauters, E., Roekens, E., van Grieken, R., Krata, A., Makarovska, Y., Maenhaut, W., Chi, X., Geypens, B., 2011. Chemkar PM10: An extensive look at the local differences in chemical composition of PM10 in Flanders, Belgium. Atmos. Environ. 45, 108–116. doi:10.1016/j.atmosenv.2010.09.040

Vu, T. V., Delgado-Saborit, J.M., Harrison, R., 2015. Review: Particle number size distributions from seven major sources and implications for source apportionment studies. Atmos. Environ. doi:10.1016/j.atmosenv.2015.09.027

Walker, S.C., Allen, S., Bell, G., Roberts, C.J., 2015. Analysis of leaf surfaces using scanning ion conductance microscopy. J. Microsc. 258, 119–126. doi:10.1111/jmi.12225

Wang, H., Shi, H., Li, Y., Yu, Y., Zhang, J., 2013. Seasonal variations in leaf capturing of particulate matter, surface wettability and micromorphology in urban tree species. Front. Environ. Sci. Technol. 1–10. doi:10.1007/s11783-013-0524-1

Wang, J., Li, S., Li, H., Qian, X., Li, X., Liu, X., Lu, H., Wang, C., Sun, Y., 2017. Trace metals and magnetic particles in PM 2.5: Magnetic identification and its implications. Sci. Rep. 7, 1–11. doi:10.1038/s41598-017-08628-0

Wang, L., Gong, H., Liao, W., Wang, Z., 2015. Accumulation of particles on the surface of leaves during leaf expansion. Sci. Total Environ. 532, 420–434. doi:10.1016/j.scitotenv.2015.06.014

Weerakkody, U., Dover, J.W., Mitchell, P., Reiling, K., 2018. Evaluating the impact of individual leaf traits on atmospheric particulate matter accumulation using natural and synthetic leaves. Urban For. Urban Green. 30, 98–107. doi:10.1016/j.ufug.2018.01.001

WHO, 2018. http://www.who.int/news-room/detail/02-05-2018-9-out-of-10-people-worldwide-breathe-polluted-air-but-more-countries-are-taking-action. Accessed 28 September 2018.

Yatkin, S., Gerboles, M., Borowiak, A., Tanet, G., Pedroni, V., Passarella, R. and Lagler, F., 2011. Evaluation of EDXRF for the determination of elements in PM10 filters, EUR 24983 EN, Publications Office of the European Union, Luxemburg.

Highlights

• Ivy and strawberry leaves followed up every three weeks for a three months period.
• Dust accumulation observed visually and magnetically, yet limited in metal built-up.
• Ivy accumulated more than strawberry, with the latter more susceptible to wash-off.
• Site-source and precipitation dynamics over time were detected by leaf biomonitoring.
• Combination of techniques assists in understanding the complex leaf-dust interaction.

Declaration of interests

☒ The authors declare that they have no known competing financial interests or personal relationships that could have appeared to influence the work reported in this paper.

☐The authors declare the following financial interests/personal relationships which may be considered as potential competing interests: